# Comparative analysis of bed resistance partitioning in high-gradient streams

Gabrielle C. L. David,[1] Ellen Wohl,[1] Steven E. Yochum,[2] and Brian P. Bledsoe[2]

Received 11 May 2010; revised 23 March 2011; accepted 4 April 2011; published 2 July 2011.

[1] Total flow resistance can be partitioned into its components of grain ($ff_{grain}$), form ($ff_{step}$), wood ($ff_{wood}$), and spill ($ff_{spill}$) resistance. Methods for partitioning flow resistance developed for low-gradient streams are commonly applied to high-gradient systems. We examined the most widely used methods for calculating each component of resistance, along with the limitations of these methods, using data gathered from 15 high-gradient ($0.02 < S_0 < 0.195$) step-pool, cascade, and plane-bed reaches in Fraser Experimental Forest. We calculated grain resistance using three equations that relate relative submergence ($R/D_m$) to $ff_{grain}$ as well as using an additive drag approach. The drag approach was also used for calculating $ff_{wood}$ and $ff_{step}$. The $ff_{grain}$ contributed the smallest amount toward all reaches at all flows, although the value varied with the method used. The Parker and Peterson (1980) equation using $D_{90}$ best represented $ff_{grain}$ at high flows, whereas the Keulegan (1938) equation using $D_{50}$ best characterized $ff_{grain}$ at base flows, giving a lower bound for grain resistance. This suggests that $ff_{grain}$ may be better represented if two grain sizes are used to calculate this component of resistance. The drag approach, which is used to calculate wood resistance, overestimated the significance of individual logs in the channel. The contribution of $ff_{spill}$ was reduced at higher flows when form drag around the step is accounted for at higher flows. We propose a method for evaluating the contribution of $ff_{step}$ that accounts for form drag around the steps once they are submerged at higher flows. We evaluated the potential sources of error for the estimation of each component of resistance. Determination of the drag coefficient was one of the major sources of error when calculating drag around wood, steps, or boulders.

**Citation:** David, G. C. L., E. Wohl, S. E. Yochum, and B. P. Bledsoe (2011), Comparative analysis of bed resistance partitioning in high-gradient streams, *Water Resour. Res., 47*, W07507, doi:10.1029/2010WR009540.

## 1. Introduction

[2] Quantifying flow resistance is essential to understanding the hydraulics of streams. Interactions between streamflow and channel boundaries dissipate energy as water moves around and over bed irregularities. Flow resistance is created by viscous skin friction around objects as well as form/pressure drag created from differential pressures around objects [*Ferguson*, 2007]. The total value of the frictional losses can be represented with the dimensionless Darcy-Weisbach friction factor:

$$ff = \frac{8gR_hS_f}{\bar{v}^2}, \tag{1}$$

where $ff$ is Darcy-Weisbach friction factor, $g$ is acceleration due to gravity (m s$^{-2}$), $R_h$ is hydraulic radius (m), $S_f$ is friction slope (m m$^{-1}$), and $\bar{v}$ is mean velocity (m s$^{-1}$).

[3] There are a number of sources of error in the calculation of $ff$ for steep channels. Each parameter ($\bar{v}$, $S_f$, $R_h$) has error associated with the measurement method [*David*, 2011]. The use of $ff$, along with Manning's $n$, nonetheless remains the most common approach to quantifying resistance in steep streams despite indications that Manning's equation in particular is poorly suited to steep streams with shallow flows [*Ferguson*, 2010].

[4] *Einstein and Barbarossa* [1952] proposed that, despite interactions among different components of resistance, the individual components could be quantified and summed. The $ff_{total}$ is commonly partitioned into its components of grain, form, and spill resistance:

$$ff_{total} = ff_{grain} + ff_{form} + ff_{spill}, \tag{2}$$

where $ff_{grain}$ is viscous friction and form drag around grains in the absence of bedforms, $ff_{form}$ is form drag around bedforms, which should not be confused with the individual component of form drag around other objects such as boulders, and $ff_{spill}$ is energy dissipation from flow acceleration and deceleration, usually over steps. *Shields and Gippel* [1995] also proposed partitioning $ff$ into the components from wood ($ff_{wood}$), banks ($ff_{banks}$), and bends ($ff_{bends}$). Extensive effort has been devoted to quantifying the

[1]Department of Geosciences, Colorado State University, Fort Collins, Colorado, USA.
[2]Department of Civil and Environmental Engineering, Colorado State University, Fort Collins, Colorado, USA.


0043-1397/11/2010WR009540

relative importance of different components of *ff* during the past few decades, yet no consensus has been reached regarding the most important components or the most appropriate method to calculate individual components. In this paper we evaluate several methods for partitioning *ff* and identify the limitations of these methods when applied to steep streams.

[5] Additive approaches have been used to investigate the contribution of grains [*Einstein and Barbarossa*, 1952; *Parker and Peterson*, 1980; *Millar and Quick*, 1994; *Millar*, 1999], wood and spill resistance [*Shields and Gippel*, 1995; *Curran and Wohl*, 2003], and bar resistance in gravel bed rivers [*Parker and Peterson*, 1980; *Prestegaard*, 1983]. *Wilcox et al.* [2006] demonstrated, however, that the unmeasurable component was always the largest contributor to total resistance, so that an additive approach inflates the leftover component. Thus, quantifying the relative contribution of different sources of resistance remains a primary challenge to understanding flow resistance in streams.

[6] A second primary challenge is to quantify the total *ff* in steep streams where the roughness elements are on the same order of magnitude as the flow depth, creating frequent wakes, jets, and standing waves, as well as spill resistance where local acceleration and deceleration occur. As discharge increases, elements may be submerged, allowing velocity to increase much faster with discharge than in low-gradient channels [*Lee and Ferguson*, 2002]. Relative submergence of a characteristic grain size ($R/D_{84}$) is commonly used to predict $ff_{\text{total}}$ [*Keulegan*, 1938; *Limerinos*, 1970; *Hey*, 1979; *Bathurst*, 1985, 1993], although this approach can have high error rates when applied to steep mountain streams [*Thorne and Zevenbergen*, 1985]. A dimensionless hydraulic geometry approach has been proposed as a more suitable method for predicting velocity in place of using a flow resistance equation in high-gradient streams [*Rickenmann*, 1991; *Ferguson*, 2007; *Zimmerman*, 2010], but it remains useful to employ a partitioning method to understand how different objects in the channel affect total flow resistance.

[7] Mountain streams with gradients $\geq 0.02$ m m$^{-1}$ have distinctive channel morphologies consisting of step-pools, cascades, and plane-bed reaches [*Montgomery and Buffington*, 1997]. Spill resistance contributes a major proportion of flow resistance in step-pool reaches [*Abrahams et al.*, 1995]. As for steep streams in general, understanding the relative contribution of different sources of resistance is challenging for step-pool channels. Most approaches are based on boundary layer theory, which assumes a semilogarithmic velocity profile, although the profile in steep streams more closely resembles an s shape [*Wiberg and Smith*, 1991].

[8] Steps create flow resistance via viscous friction over large particles, but the hydraulics of step-pool reaches indicate that the $ff_{\text{total}}$ is a function of more than just the relative submergence of a representative grain size [*Lee and Ferguson*, 2002; *Aberle and Smart*, 2003]. Deviations from the relative submergence equations are related to bed material size distribution, shape, and orientation [*Bathurst*, 2002] as well as step geometry [*Maxwell and Papanicolaou*, 2001].

[9] Step geometry is particularly important because steps create flow resistance by form drag ($ff_{\text{step}}$) from pressure differences around the upstream and downstream sides of the step and spill resistance ($ff_{\text{spill}}$) from flow acceleration and deceleration over the steps [*Chartrand and Whiting*, 2000]. Form drag varies with step geometry and composition, longitudinal step spacing, and stage [*Zimmerman and Church*, 2001; *Wilcox and Wohl*, 2006]. Spill resistance varies with step geometry, wood density, and orientation [*Comiti et al.*, 2009; *Curran and Wohl*, 2003; *Wilcox and Wohl*, 2006; *Comiti et al.*, 2008].

[10] The contribution of spill versus form resistance depends on the submergence of the step. The flow regime over a step is generally characterized as nappe flow, transition flow, or skimming flow [*Chanson*, 1994; *Church and Zimmerman*, 2007; *Comiti et al.*, 2009]. Nappe flow occurs when water free falls over a step and alternates between subcritical and supercritical flow. Nappe flow with a submerged jet is affected by the downstream tailwater [*Comiti et al.*, 2009]. Skimming flow is characterized by supercritical flow over completely submerged steps and is dominated by form resistance in the cavity recirculation [*Chanson and Toombes*, 2002].

[11] Despite the large contribution of $ff_{\text{spill}}$ in high-gradient streams, the average Froude number (*Fr*) is consistently measured as subcritical in steep streams, even at bank filling and flood flows [*Jarrett*, 1984; *Wilcox and Wohl*, 2007; *Magirl et al.*, 2009]. Skimming flow is rarely observed in step-pool systems [*Comiti et al.*, 2009]. *Grant* [1997] hypothesized that the tendency for the flow to accelerate in high-gradient streams is counterbalanced by the bedforms, which offset this tendency by dissipating energy. Regardless of local increases in velocities, the drag around boulders, bedforms, and wood maintains a subcritical range across most of a high-gradient mountain stream.

[12] Wood resistance in step-pool channels is related to the effect of individual pieces ($ff_{\text{wood}}$) and to wood as part of the step form ($ff_{\text{step}}$) [*Curran and Wohl*, 2003]. Parameters such as spatial density of wood, orientation, length, and position significantly affect the drag coefficient [*Young*, 1991; *Gippel et al.*, 1992; *Wallerstein et al.*, 2002] and the contribution of wood to total resistance, which is also influenced by discharge [*Wilcox and Wohl*, 2006].

[13] In quantifying grain resistance, most studies use some form of the *Keulegan* [1938] equation:

$$ff_{\text{grain}} = \left[2.03 \log\left(\frac{12.2R_h}{k_s}\right)\right]^{-2}, \tag{3}$$

where $k_s$ is a multiple of a characteristic grain diameter. The values for $k_s$ are typically some multiple of $D_{50}$, $D_{84}$, or $D_{90}$ [e.g., *Parker and Peterson*, 1980; *Griffiths*, 1989; *Millar*, 1999]. Grain resistance is most often defined as the viscous friction around grains, but in high-gradient channels, where boulders are on the same order of magnitude as flow depth, the grains can contribute significantly to form drag and spill resistance [*Zimmerman*, 2010]. Grain resistance is defined here as the combined flow resistance (i.e., form drag, skin friction, spill resistance) that results from the presence of the grains in the flow.

[14] *Baiamonte and Ferro* [1997] suggest that total resistance is a function of *Fr*, the Reynolds number (*Re*), concentration of coarser elements ($\Gamma$), *Shields* [1936] parameter ($\tau^*$), and measures of longitudinal and transverse

distance between roughness elements. The concentration of coarser elements is found using

$$\Gamma = \frac{N_B \pi D_B^2}{4WL}, \quad (4)$$

where $N_B$ is number of boulders on the chute placed over the entire surface of the chute and $D_B$ is median size of boulders. Analogous to step spacing, spatial density of boulders maximizes flow resistance at a concentration between 0.15 and 0.40 [*Rouse*, 1965; *Canovaro et al.*, 2007] and can be the main factor affecting flow resistance [*Pagliara and Chiavaccini*, 2006].

[15] As noted above in the discussion on steps, the relationship between *Fr* and drag around an object is complex, depending on the relative submergence of the object. *Fr* is related to the drag coefficient. *Fr*, combined with the size and spacing of the roughness elements, influences the relative contribution of the free surface drag. Peak drag occurs when *Fr* is between 0.5 and 0.6 and the relative submergence is greater than 0.8 [*Bathurst*, 1982]. The relationship between *Fr* and total drag on the bed means that the boulder concentration is needed to represent flow resistance from bed elements [*Bathurst*, 1982]. $ff_{\text{total}}$ is inversely related to *Fr* [*Ferro*, 2003].

[16] Understanding the contributions of different sources of roughness in steep streams will improve our ability to calculate $ff_{\text{total}}$ in these channels, which is essential for the prediction of velocity and discharge. Velocity and discharge predictions are in turn used by engineers for fish-habitat assessments, stream rehabilitation projects, flood estimation, and sediment routing models [*Bathurst*, 2002; *Ferguson*, 2007]. Despite some success in using dimensionless hydraulic geometry equations to predict velocity and discharge in high-gradient streams [*Zimmerman*, 2010], we need to improve our understanding of how individual components affect the flow. Consequently, the following analysis focuses on the most commonly used methods for partitioning flow resistance. The primary objectives of this paper are as follows:

[17] 1. Evaluate methods for calculating $ff_{\text{grain}}$, $ff_{\text{wood}}$, and $ff_{\text{step}}$ using a data set from 15 steep stream reaches with step-pool, cascade, and plane-bed morphology.

[18] 2. Identify limitations in the existing methods of calculating total and component resistance when these methods are applied to steep streams.

[19] The analyses presented here ignore bank roughness and associated resistance. Although this may be an important source of resistance in steep streams, these analyses follow the precedent of earlier papers in focusing on bed configuration.

## 2. Field Area

[20] East St. Louis Creek (ESL) and Fool Creek (FC) are located at elevations of 2900–3900 m in Fraser Experimental Forest in the Rocky Mountains of Colorado, 112 km west-northwest of Denver (Figure 1). Runoff is dominated by snowmelt with small contributions by summer convective storms. Average annual precipitation over the entire forest is 787 mm (USDA Forest Service, About Fraser Experimental Forest, http://www.fs.fed.us/rm/fraser/ about/ index.shtml, accessed September 1, 2009). Peak discharges occur in mid-June with 80% of the total flows occurring between April and October [*Wilcox and Wohl*, 2007].

[21] ESL drains approximately 8.73 km$^2$ and has been gauged since 1943. The Fool Creek basin (LFC) drains 2.89 km$^2$ and has been gauged since 1941. The upper portion of Fool Creek basin (UFC) drains 0.69 km$^2$, with a gauge installed circa 1986. All of the basins are dominated by cascade and step-pool morphologies above the gauges, with limited plane-bed reaches.

[22] Step-pool reaches in both ESL and LFC include large amounts of wood, over 95% of which is found in the steps. Most of the step-pool reaches have about half the steps formed of boulders and half created by a wood jam around one large keystone boulder. Cascade reaches were selected based on visual assessment of tumbling flows over irregularly spaced clasts, with no or limited regular sequences of steps and pools and small or underdeveloped pools.

## 3. Methods

### 3.1. Field Methods

[23] Fifteen channel reaches on ESL and FC were selected based on visual assessment of morphology; nine step-pool, five cascade, and one plane-bed reach. Upper and lower boundaries of each reach were chosen to ensure consistent morphology and gradient within the reach. Reaches are labeled in order from downstream to upstream on each basin (Figure 1).

[24] A laser theodolite was used to collect bed and water surface data every 15 cm along the thalweg and banks of each reach. All measurements were made over two summers in 2007 and 2008. The water surface was surveyed during a high flow (June 2008), two intermediate flows (July 2007 and 2008), and one low flow (August 2007). These four measurement periods are referred to as flow periods in the rest of the paper. During each of these surveys the reach-average mean velocity was measured using Rhodamine WT dye tracer and fluorometers attached to rebar, a metal rod $\sim$1/4 inches in diameter, fixed in the thalweg of the streambed at the upstream and downstream end of each reach. Despite the lack of a logarithmic velocity profile, the reach-average mean velocity can still be approximated by placing probes at 0.6$h$ or 0.2$h$ and 0.8$h$, where $h$ is flow depth from the water surface [*Wiberg and Smith*, 1991; *Legleiter et al.*, 2007; *Wilcox and Wohl*, 2007]. The probes recorded values at 1-second intervals until the values returned to background levels. Measurements were repeated four times in each reach at each flow period. The differences between the centroids of the mass of dye were used for determining the time difference between the two probes [*Calkins and Dunne*, 1970; *Lee and Ferguson*, 2002]. The range of discharges, *Fr*, *Re*, and dimensionless unit discharge ($q^*$) measured are summarized for each flow period in Table 1.

[25] The intermediate axis of each of 300 clasts in each reach was measured with a ruler. Clasts were measured at evenly spaced cross sections throughout the reach, which were anywhere from 0.5 to 1 m apart, to create a composite count for each reach. The locations of the cross sections were surveyed so that the data could subsequently be split based on where the clasts were located in the reach (step, upstream pool, downstream pool, cascade section, step tread).

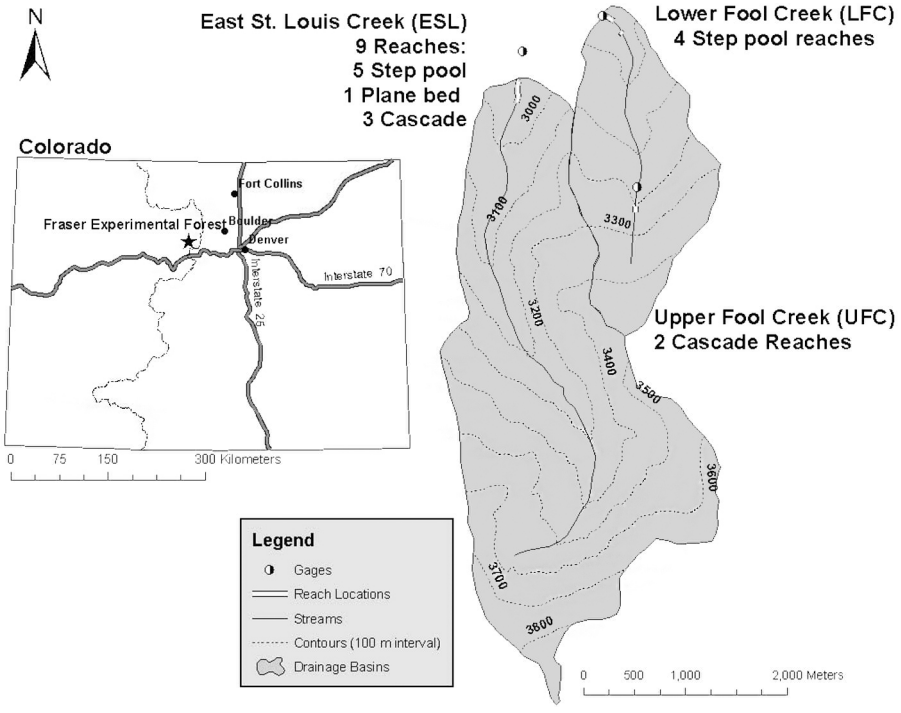


**Figure 1.** Location map for Fraser Experimental Forest.

[26] A tripod-mounted light detection and ranging (LiDAR) Leica HDS Scanstation was used during the August 2007 low-flow period to capture bank and bed topography. The LiDAR scans were coupled with a feature based survey with variable gridding that depended upon the underwater features, which was completed with a laser theodolite. The water surface data were imported into the scans and used together with cross sections created in Cyclone 5.8.1 [*Leica Geosystems*, 2008] using the LiDAR scans to calculate channel geometry data; i.e., width ($w$), depth ($h$), hydraulic radius ($R_h$), and cross-sectional area ($A$). Values of these variables were reach averages based on multiple cross sections.

[27] The step-forming material of boulders or wood was identified for each step in the step-pool reaches: a boulder grouping indicates only boulders; wood1 indicates wood surrounding a keystone boulder; wood2 indicates only wood with no evident keystone boulder. The majority of wood was found in the steps in almost every reach, except for the cascade and plane-bed reaches. Individual pieces made up a small amount of the wood found in each reach. As the stage went down many of these logs were no longer within the flow, further reducing the contribution of $ff_{\text{wood}}$ to $ff_{\text{total}}$.

[28] Wood length and diameter were measured for each flow period using a combination of the LiDAR scans, a TIN (triangulated irregular network) of the water surface created in Cyclone 5.8.1, and photographs. The wood volume was calculated from these measurements and divided by the plan area of the reach ($L_r$*$w$, where $L_r$ is reach length and $w$ is average width). Reach lengths varied between 6.4 m (ESL6) and 35.5 m (ESL8). A more detailed description of methods as well as a detailed table showing all the values measured for each reach at each flow period can be found in *David* [2011] and *David et al.* [2010a].

### 3.2. Partitioning Methods

[29] *Einstein and Barbarossa* [1952] introduced the concept of dividing shear stress into the two components of shear applied to grains in channels without bedforms ($\tau_0'$) and shear applied to bedforms ($\tau_0''$):

$$\tau_0 = \tau_0' + \tau_0'', \tag{5}$$

**Table 1.** Summary Values for Discharge ($Q$), Dimensionless Unit Discharge ($q^*$), Froude Number ($Fr$), and Reynolds Number ($Re$) for Each Flow Period[a]

| Flow Period | $Q$ ($m^3\ s^{-1}$) | $R/D_{50}$ | $R/D_{84}$ | $q^*$ | $Fr$ | $Re$ |
|---|---|---|---|---|---|---|
| Aug 2007 (low) | 0.01–0.18 | 1.01–21.92 | 0.52–2.18 | 0.09–0.88 | 0.12–0.33 | $5.5 \times 10^3$–$5.6 \times 10^4$ |
| Jul 2007 (intermediate) | 0.02–0.34 | 1.54–28.24 | 0.79–2.81 | 0.27–1.87 | 0.20–0.42 | $1.5 \times 10^4$–$9.8 \times 10^4$ |
| Jul 2008 (intermediate) | 0.02–1.13 | 1.54–29.35 | 0.79–2.92 | 0.25–5.08 | 0.15–0.86 | $1.5 \times 10^4$–$3.0 \times 10^5$ |
| Jun 2008 (high) | 0.10–1.85 | 2.38–35.24 | 1.22–3.83 | 0.80–7.92 | 0.27–0.97 | $6.2 \times 10^4$–$3.8 \times 10^5$ |

[a]The values represent the range measured for all the reaches during each subsequent flow period. Dimensionless unit discharge is defined as $q/\sqrt{(gD_{84}{}^3)}$, where $q = Q/w$.

where $\tau_0$ is total boundary shear stress. *Einstein and Barbarossa* [1952] applied the method by partitioning the hydraulic radius, but in this case the slope is being partitioned similar to *Millar* [1999]. The Darcy-Weisbach friction factor can then be related to equation (5) by

$$ff = 8\left(\frac{\sqrt{\tau_0/\rho}}{\bar{v}}\right)^2, \tag{6}$$

where $\bar{v}$ is mean flow velocity and $\rho$ is density of water. Each component of shear stress (equation (5)) can be substituted into equation (6) to yield the component value of *ff*. The values of the component friction factor are then substituted back into equation (2). The shear stress applied to each object can be determined by considering the drag force applied to grains, wood, or steps in the channel. The total drag force includes both viscous and form effects:

$$F_D = C_D\rho\frac{\bar{v}^2}{2}A_F, \tag{7}$$

where $F_D$ is drag force; $C_D$ is coefficient of drag, and $A_F$ is frontal area of object in flow. The shear applied to that object is then found by dividing the drag force by the area the force is applied over:

$$\tau_0 = \frac{F_D}{A_{\text{channel}}}, \tag{8}$$

where $A_{\text{channel}}$ is surface area force applied over

$$ff_D = \frac{8\tau_0}{\rho\bar{v}^2} = \frac{4C_DA_F}{W*L}, \tag{9}$$

where $W$ is width, $L$ is length that force is applied over, and $ff_D$ is friction factor for individual component.

[30] The total friction factor ($ff_{\text{total}}$) is calculated using equation (1) and substituting water surface slope ($S_w$) for friction slope ($S_f$). The water surface slope was calculated using the slope of the regression line of the longitudinal survey of the thalweg.

### 3.2.1. Grain Resistance

[31] Of several methods for predicting the portion of resistance related to grains, the most commonly used is the *Millar and Quick* [1994] adaptation of the *Keulegan* [1938] equation which uses $D_{50}$ as the characteristic grain size:

$$ff_{\text{grain}} = 8*\left[2.5\ln\left(\frac{12.2R_h}{D_{50}}\right)\right]^{-2}. \tag{10}$$

[32] This equation provides a lower bound for grain resistance that better represents small-scale roughness in deep flows [*Millar*, 1999]. Variants on equation (10) include those developed by *Parker and Peterson* [1980],

$$ff_{\text{grain}} = 8*\left[2.5\ln\left(\frac{11R_h}{2D_{90}}\right)\right]^{-2}, \tag{11}$$

and a power law relation by *Bathurst* [2002],

$$ff_{\text{grain}} = 8*\left[3.1\left(\frac{R_h}{D_{84}}\right)^{0.93}\right]^{-2}. \tag{12}$$

[33] For this data set the average $D_{50}$, as well as the step tread $D_{50}$, were used to analyze the effect of grain resistance and to evaluate sensitivity of the results to sampling location. Because the steps are assumed to create their own form of resistance, step $D_{50}$ was not used to calculate $ff_{\text{grain}}$. The *Bathurst* [2002] equation is similar to an equation proposed by *Ferguson* [2007] for shallow flows, except the exponent is 1 and the coefficient is 2.5 in the latter equation.

[34] Additive partitioning can only be used if boulders are sufficiently far apart that the wake of one boulder does not interfere with the next boulder [*Ferro*, 2003]. When depth is on the same order of magnitude as the bed material height ($R/D_{84} < 4$), flow resistance has to be determined from drag forces on boulders rather than from the boundary layer theory [*Bathurst*, 1993]. Therefore, the drag force approach, described above, was used for individual boulders. Significant clasts were identified as those above the water surface at low flows, which were thus included in the LiDAR scans. If the boulders were too closely spaced (length to height ratio <9.0 [*Wohl and Ikeda*, 1998]), so that wake interference occurred between boulders, the width and representative height of clusters of boulders were used in place of individual boulders. Although the drag coefficient may be closer to 0.9 [*Nelson et al.*, 1993] in streams with large relative roughness, a drag coefficient of 0.4 was used for each boulder as well as clusters of boulders based on the classic Reynolds number drag relationship that represents a sphere in a free stream [*Wiberg and Smith*, 1991; *Lawrence*, 2000]. The Reynolds number remained between $10^4$ and $10^5$ for all flow periods in all streams except for FC3, FC5, and FC6 at low flow. Because the Reynolds number indicates fully turbulent flows in all reaches except the three Fool Creek reaches, the same drag coefficient is used at both low and high flows. FC3, FC5, and FC6 are given a value of 0.6 for the drag coefficient based on the Reynolds number at low flows. The length is the length ($L$) between boulders, and the width ($W$) is the wetted width of the cross section where the boulders were located (equation (9)). The frontal area for a fully submerged hemispherical particle is $A_F = 1/2\Pi k^2$, where $k$ is the radius of the particle. The frontal area of a partially submerged particle is $A_F = 2kh$, where $h$ is flow depth [*Lawrence*, 1997]. At low flow the wake effect between particles was not considered to be as large, therefore a value of $ff_{\text{grain}}$ based on the drag force approach was calculated for each individual particle rather than for clusters of clasts. This method was used as a means of comparing the additive partitioning of the drag force for individual large bed elements against the other methods of calculating $ff_{\text{grain}}$.

[35] Grain resistance is commonly calculated using a form of the *Keulegan* [1938] equation (equations (10) and (11)), which is based on the assumption that velocity varies with depth in a logarithmic fashion [*Wiberg and Smith*, 1991; *Bathurst*, 2002]. The *Bathurst* [2002] equation (equation (12)) is the only equation tested here that is based on a power law relation rather than assuming a logarithmic velocity distribution. The three equations (*Bathurst* [2002],

*Parker and Peterson* [1980], and *Keulegan* [1938]) are tested against an additive drag force approach. Errors associated with the calculation of grain resistance involve accurately measuring the hydraulic radius and the grain size. Pebble counts were used to calculate reach average $D_{84}$, $D_{50}$, and $D_{90}$ as well as values for the steps, step treads, cascading sections, and upstream and downstream pools. Because the objective is to separate grain resistance from $ff_{\text{step}}$, we assume that the grains on the step treads have the greatest influence on grain resistance and best characterize the $ff_{\text{grain}}$ in the step-pool reaches. The step grain size may be appropriate for predicting total resistance in a step-pool channel [*Lee and Ferguson*, 2002], but here the step-forming grains are considered part of $ff_{\text{step}}$ and $ff_{\text{spill}}$. The cascade reaches did not have step treads, therefore the $D_{84}$ and $D_{50}$ were split into cascade sections and pool sections. The root-mean-square error (RMSE) was used to evaluate the goodness of fit between the predicted *ff* based on the different grain sizes for the reach and the step tread.

[36] Each of the above methods was further evaluated by regressing $ff_{\text{grain}}$ against the value of $ff_{\text{grain}}$ from the drag approach. The total resistance ($ff_{\text{total}}$) was transformed using the square root to meet regression assumptions of homoscedacity [*Kutner et al.*, 2005].

#### 3.2.2. Wood Resistance ($ff_{\text{wood}}$)

[37] Here $ff_{\text{wood}}$ represents individual pieces of wood in the channel that are not part of steps. The majority of wood in step-pool reaches is found within the steps (~90%), but that wood is considered part of the step form and its contribution to $ff_{\text{total}}$ is considered a part of $ff_{\text{step}}$ and $ff_{\text{spill}}$.

[38] The contribution of individual pieces of wood was calculated using the method outlined by *Wilcox et al.* [2006]. The major assumption is that the drag created by wood is similar to the drag measured around cylinders in a flume [*Gippel et al.*, 1992; *Shields and Gippel*, 1995; *Gippel et al.*, 1996]. The drag force around wood is

$$F_D = \frac{\rho C_D^{\text{app}} \bar{V}^2 A_w \sin\theta}{2}, \tag{13}$$

where $C_D^{\text{app}}$ is apparent drag coefficient (measured for a specific set of geometric and hydraulic conditions and corrected for the blockage effect of wood), $\bar{V}$ is depth-averaged approach velocity, $A_w$ is submerged cross-sectional area of the wood piece, and $\theta$ is angle of the wood piece relative to downstream thalweg. The apparent drag coefficient is then

$$C_D^{\text{app}} = \frac{C_D}{a(1-B)^b}, \tag{14}$$

where $C_D$ is drag coefficient in flow without boundary effects, $a$ and $b$ is empirically derived coefficient and exponent, and $B$ is blockage ratio. For values of $B$ between 0.03 and 0.4 the values of $a$ and $b$ equal 1 and 2, respectively. The blockage ratio is the ratio of the frontal area of an object to the cross-sectional area of flow. For a cylindrical piece of wood

$$B = \frac{L' d_{\text{wood}} \sin\theta + \pi\left(\frac{d_{\text{wood}}}{2}\right)^2 \cos\theta}{A_{\text{flow}}}, \tag{15}$$

where $L'$ is piece length, $d_{\text{wood}}$ is submerged cylinder diameter, and $A_{\text{flow}}$ is cross-sectional area of the flow. Once the drag force is determined for an individual piece of wood, the shear stress can be calculated using

$$\tau_{\text{wood}} = \frac{\rho C_D^{\text{app}} \bar{V}^2 d_{\text{wood}}}{2X}, \tag{16}$$

where $X$ is distance between an upstream object producing appreciable wake and downstream log. Equation (17) can then be used to calculate the component of $ff_{\text{total}}$ related to individual pieces of wood:

$$ff_{\text{wood}} = \frac{8\tau_{\text{wood}}}{\rho \bar{V}^2} = \frac{4 C_D^{\text{app}} d_{\text{wood}}}{X}. \tag{17}$$

[39] This method eliminates the need to measure approach velocities. The minimum and maximum values used in each reach for $C_D$, $C_D^{\text{app}}$, $B$, $a$ and $b$, and the resultant $ff_{\text{wood}}$ are shown in Table 2. The values of $B$ exceed the range evaluated by *Gippel et al.* [1992] in a few cases. Values of coefficient $a$ and exponent $b$ in equation (14) were determined based on the range of $B$ measured by *Gippel et al.* [1992], and were generally 0.997 and 2.06, respectively.

#### 3.2.3. Form Resistance ($ff_{\text{step}}$)

[40] Because the main bedforms in the steep stream reaches examined here are steps and pools, the form resistance will be denoted as $ff_{\text{step}}$ rather than $ff_{\text{form}}$. Other sources of form resistance are considered separately as $ff_{\text{wood}}$ and $ff_{\text{spill}}$. Form resistance related to banks, bends, and sinuosity is important, but is not calculated here since the primary focus is the contribution from bed roughness toward total flow resistance. Other components of resistance are folded into spill resistance ($ff_{\text{spill}}$).

[41] Much of the energy loss associated with steps and pools is related to the flow acceleration and deceleration as water spills over the step lip into the pool (Figure 2). During nappe flow the majority of the energy loss is from flow recirculation in the pool. If the drop is not shear, a hydraulic jump dissipates the energy. As a step becomes submerged during higher flows, the step shape itself may also create losses from form resistance. The step submergence can be evaluated using the ratio of critical depth ($h_c$) to drop height ($z$) (Figure 2). *Comiti et al.* [2009] found a transition in the significance of grain resistance versus spill resistance at a value of $h_c/z$ of 1.2. Consequently, we hypothesize that steps with a value of $h_c/z > 1.2$ should also have a form resistance component ($ff_{\text{step}}$) related to the step shape. We evaluated step submergence based on longitudinal profiles and photographs. The portion of *ff* related to steps can be calculated using a methodology similar to

**Table 2.** Minimum and Maximum Values Used for Each Log in Each Reach

| Parameters | Minimum | Maximum |
|---|---|---|
| $C_D$ | 0.2 | 1 |
| $B$ | 0.01 | 0.63 |
| $a$ | 0.997 | 1.02 |
| $b$ | 2.06 | 3.25 |
| $C_D^{\text{app}}$ | 0.2 | 4.75 |
| $ff_{\text{wood}}$ | 0.01 | 4.43 |

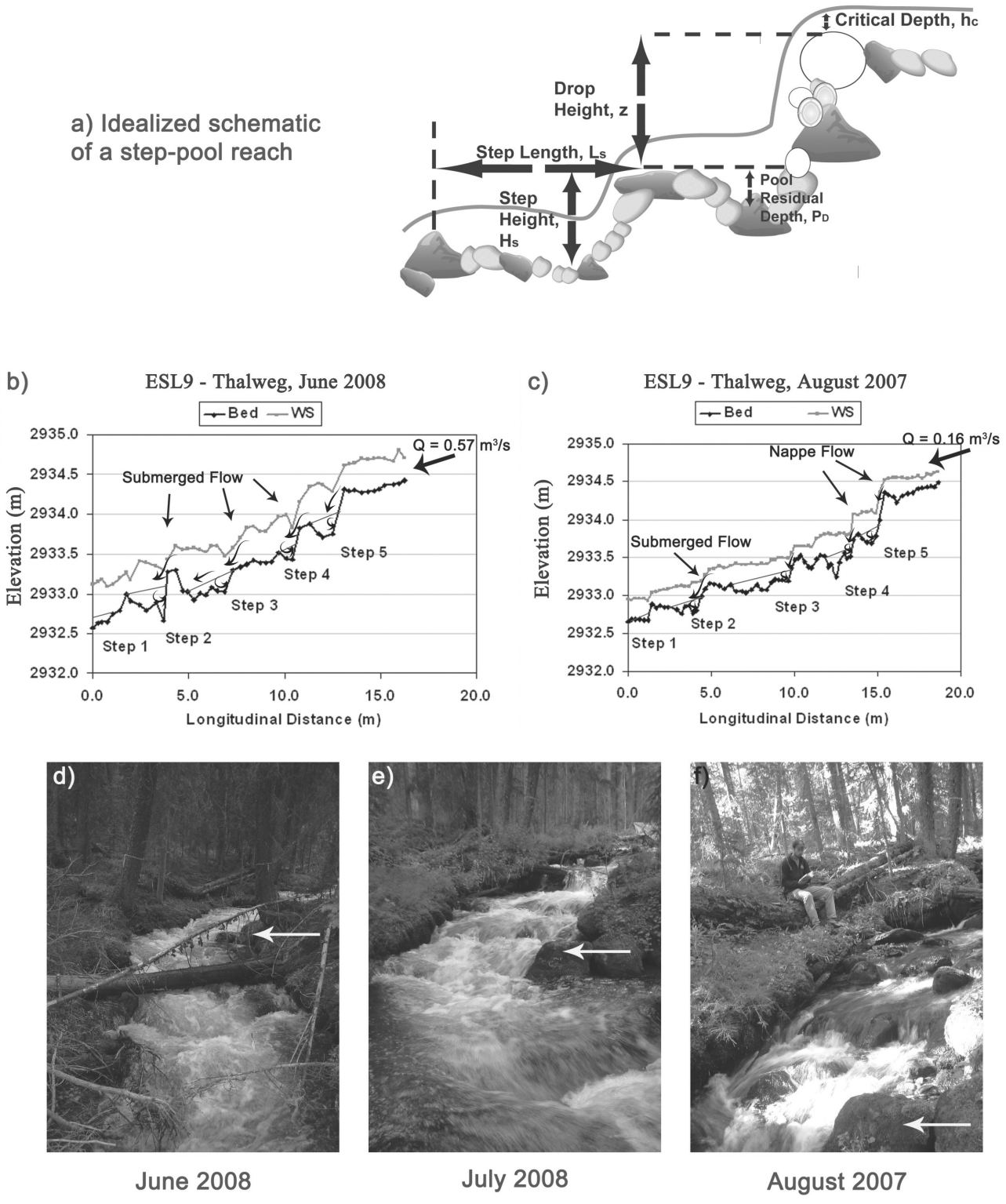


**Figure 2.** (a) Schematic of an idealized wood and boulder step-pool reach showing step height, drop height, pool depth, step length, and critical depth. (b) Longitudinal profile of a step-pool reach (ESL9) at high flow. (c) Longitudinal profile of the same step-pool reach at low flow. The distances vary between Figures 2b and 2c because the main flowpath tended to be more sinuous during low flows. The pools are shown by a flat line drawn over the pool area in each longitudinal profile. (d) A photograph looking upstream at ESL9 during high flow. (e) A photograph of ESL9 during intermediate flow. (f) A photograph of ESL9 during low flow. The white arrows point to the same rock on each picture. Notice that steps become more distinct as flow decreases.

calculating drag around in-channel wood:

$$ff_{\text{step}} = \frac{4C_D A_{\text{step}}}{A_{\text{channel}}}, \quad (18)$$

where $C_D$ is drag coefficient of steps, $A_{\text{step}}$ is frontal area of step, and $A_{\text{channel}}$ is surface area of step. The frontal area of the step was the product of the upstream pool depth ($P_D$) and width ($P_w$).

[42] Drag coefficients of steps were estimated based on the step composition; i.e., boulder, wood1, or wood2. Values were based on results from flumes [*Gippel et al.*, 1992; *Hygelund and Manga*, 2003] for individual cylinders (between 0.4 and 4.5) and results for a wood jam (between 2.6 and 9.0) [*Manners et al.*, 2007]. Because drag coefficients increase with dimensionless wood surface area [*Manners et al.*, 2007], initial values for the drag coefficient were assigned based on values of wood surface area/channel surface area [*David*, 2011]. Boulder steps were given an initial value of 1.0 for $C_D$, and wood1 and wood2 steps were given initial values between 2.8 and 1.4. A limitation of this method is the lack of measured drag coefficients around wood and boulder steps. Because the drag coefficients were unknown, a sensitivity analysis was performed. The initial value of $C_D$ was assigned for each step as described above, and then each drag coefficient was increased by 0.2 in five increments to calculate six different values of $ff_{\text{step}}$, starting with a conservative estimate for the drag coefficients. The value of $ff_{\text{step}}$ was calculated for each individual step that is submerged according to the value of $h_c/z$ using the drag force approach described above (equations (5)–(9)) and then summed to give the total value of $ff_{\text{step}}$ for each reach. The cascade reaches typically included one or two steps within the reach, but only a few of these steps were sufficiently submerged to have values for $ff_{\text{step}}$ as well.

## 4. Results

### 4.1. Grain Resistance ($ff_{\text{grain}}$)

[43] The variety and distribution of grain sizes can have a large effect on grain resistance, particularly in step-pool reaches, depending on where grains are measured within a reach. The step-pool reaches tend to have much larger variability in grain size than the cascade reaches (Figure 3), probably because of the larger range in gradient and morphology. The variability in $D_{50}$ between sections of a reach was much larger than the variability in $D_{84}$, indicating that $D_{84}$ may better represent average grains protruding above the bed for the entire reach. The grain size in the downstream pools and on the steps varied the most from the reach $D_{84}$ (Figure 3). Figure 4 shows a sensitivity analysis of each of the three grain resistance equations using $D_{50}$, $D_{84}$, and $D_{90}$ for the characteristic grain size. The values of $ff_{\text{grain}}$ using a reach grain size are compared against the values using a characteristic grain size for the step tread. The *Parker and Peterson* [1980] equation varies the least (RMSE = 0.06), whereas the *Bathurst* [2002] equation varies the most (RMSE = 0.115) (Figure 4). Results from the *Keulegan* [1938] equation using both $D_{50}$ and $D_{84}$ are fairly similar (RMSE = 0.012 and 0.018, respectively).

[44] Figure 5 illustrates the percent contribution of $ff_{\text{grain}}$ to $ff_{\text{total}}$ for each equation at low and high flows. The June 2008 mean value for $ff_{\text{grain}}$ calculated with any of the equations and using either the step tread or reach average grain size was always significantly less than the August 2007 mean value of $ff_{\text{grain}}$ (Figure 6). Therefore, in the following analysis comparisons focus on differences between June 2008 and August 2007 flows. The $ff_{\text{grain}}$ calculated from the *Keulegan* [1938] equation contributes the smallest amount toward $ff_{\text{total}}$ at both low and high flows, indicating that it gives a lower bound of grain resistance. The use of the *Keulegan* [1938] equation in these channels is similar to applying the Manning's equation to intermediate- and large-scale roughness, indicating that $ff_{\text{grain}}$ calculated with *Keulegan* [1938] best represents a lower bound of resistance in these steep, rough channels during deep flows. The percent contribution of $ff_{\text{grain}}$ is largest when calculated using the *Parker and Peterson* [1980] equation at high flows and the *Bathurst* [2002] equation at low flows. These equations are similar, since each uses a larger representative grain size and calculates an average value of $ff_{\text{grain}}$. The *Keulegan* [1938] equation calculates slightly larger values of $ff_{\text{grain}}$ based on $D_{84}$ instead of $D_{50}$ (Figure 4), but not as large as the *Parker and Peterson* [1980] or *Bathurst* [2002] relations.

[45] The $ff_{\text{grain}}$ calculated with the *Parker and Peterson* [1980] equation occasionally contributes up to 100% of total resistance at high flows in the plane-bed reach (ESL6; Figure 5). Since the $ff_{\text{wood}}$ also increases at high flow in this reach and contributes to $ff_{\text{total}}$, the *Parker and Peterson* [1980] equation is likely inflating the value of $ff_{\text{grain}}$. Therefore the *Parker and Peterson* [1980] equation may be an overestimate of $ff_{\text{grain}}$ at high flows.

[46] As grains become submerged, we expect the contribution of $ff_{\text{grain}}$ to total resistance to decrease. Although the values of $ff_{\text{grain}}$ increase at lower flows (Figure 6), the relative contribution of $ff_{\text{grain}}$ to $ff_{\text{total}}$ is much smaller at low flows for each of the three equations except for the drag force approach (Figure 5). The means vary between 0.11 and 0.08 from low to high, respectively, for the *Keulegan* [1938] equation and from 0.58 to 0.24 for the Parker and Peterson equation. In no case do the values $ff_{\text{grain}}$ go above 2.0 when using any of the three equations, despite drastic increases in $ff_{\text{total}}$ up to 42.0 during low flows. Therefore many of these equations may be underestimating $ff_{\text{grain}}$ at all flows, but more specifically at low flows.

[47] Figure 5 also displays the results of the additive drag approach for individual boulders. The percent contribution of $ff_{\text{grain}}$ to $ff_{\text{total}}$ is much larger when $ff_{\text{grain}}$ is calculated in this manner for both the June 2008 flows and the August 2007 flows. ESL7 has a percent of $ff_{\text{total}}$ greater than 100 for the drag approach, indicating that this value is unrealistic. The high values in ESL7, ESL8, and ESL9 reveal problems with using the drag approach during lower flows. Each of these three reaches has the largest number of boulders (23–28, compared to other reaches that only had 5 or 6). The additive approach causes the significance of $ff_{\text{grain}}$ to be inflated because of the number of boulders. Both ESL8 and ESL9 are step-pool reaches that have a large contribution from $ff_{\text{step}}$, $ff_{\text{wood}}$, and $ff_{\text{spill}}$. Therefore the percent contribution of $ff_{\text{grain}}$ is too high for these reaches once other sources of resistance are considered from field observations and the analysis below. Alternatively, the high values of $ff_{\text{grain}}$ calculated around individual grains that are not step-forming reveal that $ff_{\text{grain}}$ may be

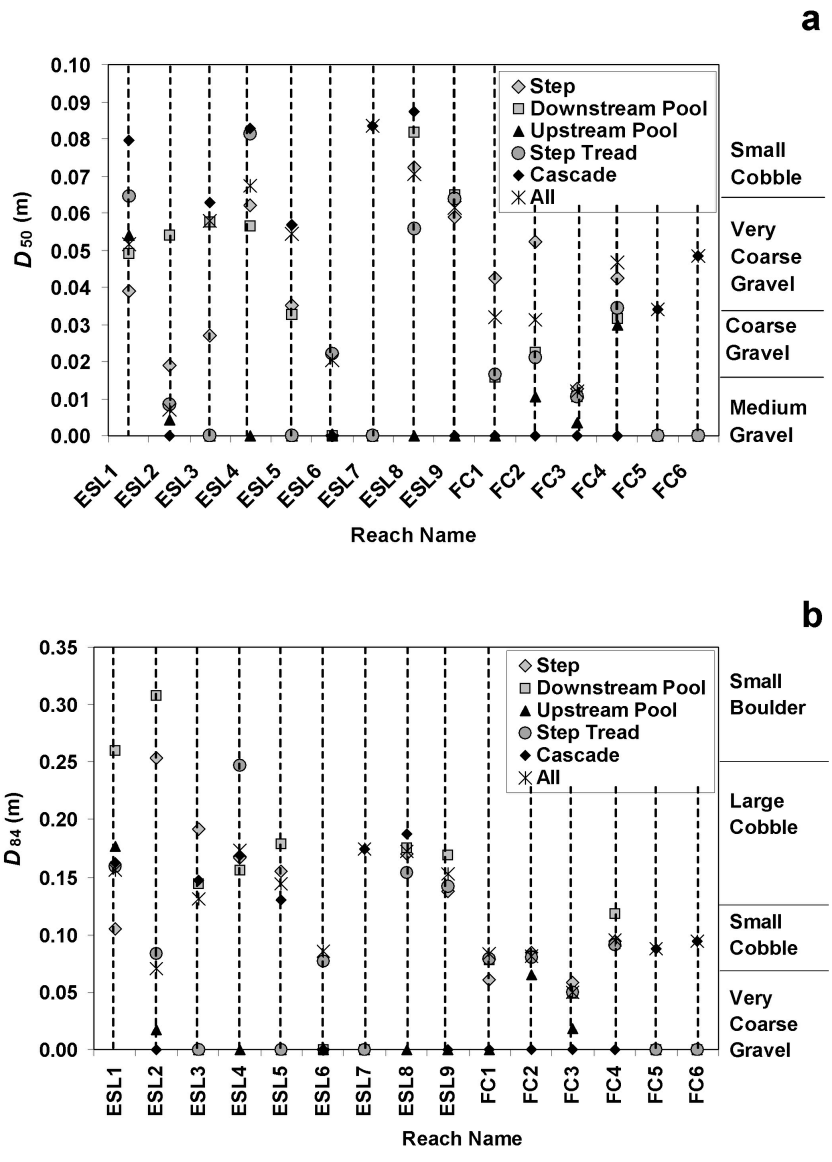


**Figure 3.** Separated (a) $D_{50}$ and (b) $D_{84}$ for each reach, illustrating the range in values, depending on the portion of the bed measured. Dotted lines are drawn through the step-pool reaches. Step $D_{84}$ RMSE = 0.061; downstream pool $D_{84}$ RMSE = 0.079; upstream pool $D_{84}$ RMSE = 0.045; step tread $D_{84}$ RMSE = 0.025. Step $D_{50}$ RMSE = 0.014; downstream pool $D_{50}$ RMSE = 0.018; upstream pool $D_{50}$ RMSE = 0.018; step tread $D_{50}$ RMSE = 0.010.

greatly underestimated in these reaches by using the *Keulegan* [1938], *Bathurst* [2002], or *Parker and Peterson* [1980] equations.

[48] The regressions used to evaluate each method of $ff_{grain}$ versus $ff_{total}$ are presented in Tables 3 and 4. The *Parker and Peterson* [1980] and *Keulegan* [1938] equations using $D_{90}$ and step tread $D_{50}$, respectively, explained the most variability in the data set. All iterations except two showed a significant difference in $ff_{grain}$ between June 2008 and August 2007 flows. Although a regression analysis reveals which equation explains a larger percentage of the variability in $ff_{total}$, it does not necessarily reveal which equation best calculates $ff_{grain}$.

[49] Each method was evaluated against the drag approach ($ff_{drag}$), assuming that the drag approach can show precise trends in the data without the values necessarily being accurate. The trends may be more precise with the drag approach because every large bed element that was above the surface during the August 2007 flows was accounted for. The regression analysis shows that the $ff_{grain}$ values from the *Keulegan* [1938] relations using the $D_{50}$, step tread $D_{50}$, and $D_{84}$ were all significantly related to the $ff_{grain}$ values from the drag approach during the June 2008 flows. None of the intercepts were significant in any of the regressions. Only the *Keulegan* [1938] step tread $D_{50}$ and *Keulegan* [1938] $D_{84}$ were significantly related to $ff_{drag}$ at low flows.

[50] Despite these differences in values, the *Keulegan* [1938], *Bathurst* [2002], and *Parker and Peterson* [1980] relations show similar trends (Figure 6). Each equation was evaluated by significant differences in the value of $ff_{grain}$ among channel types, flow period, and dominant

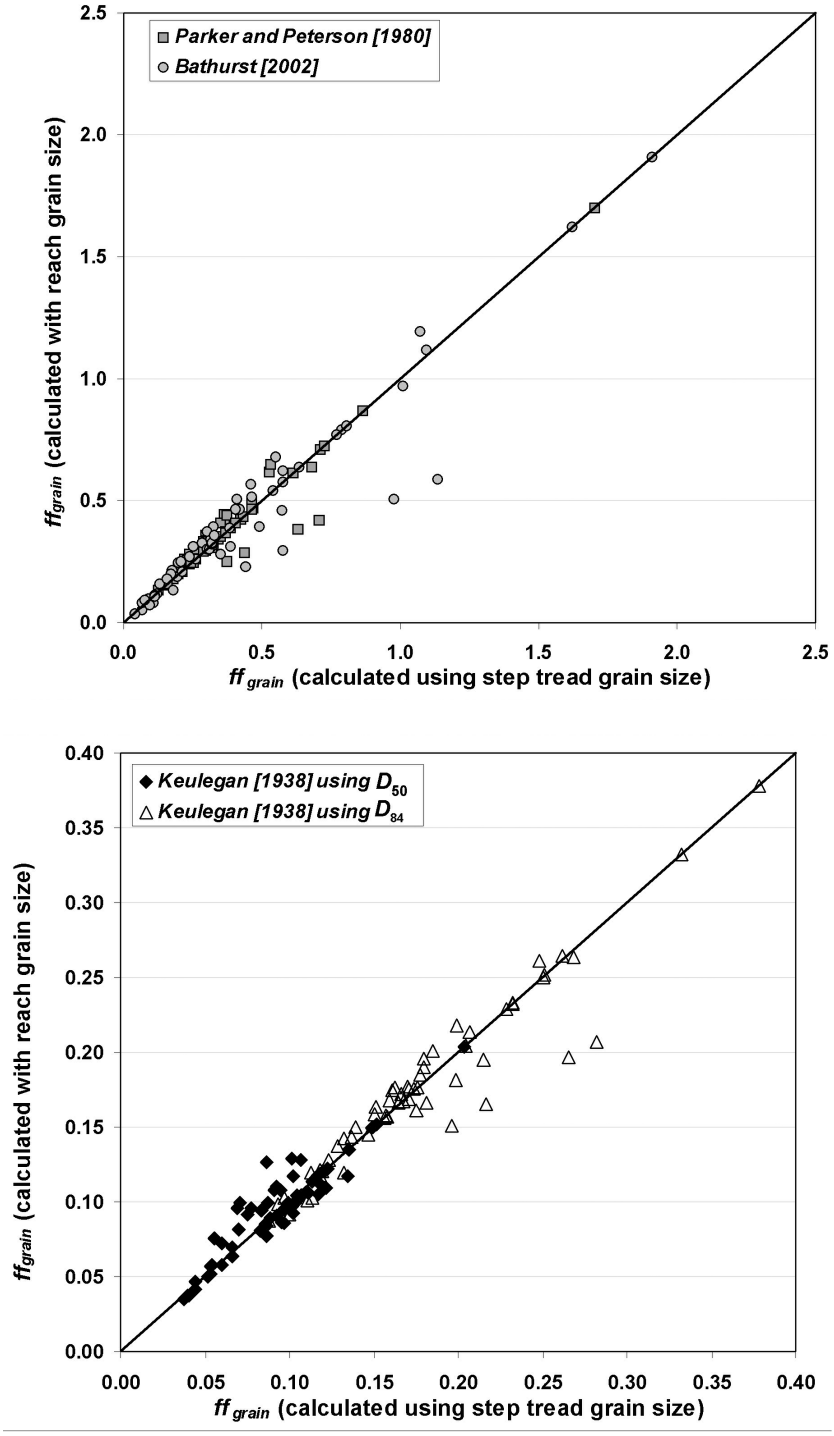


**Figure 4.** Sensitivity analysis using reach $D_{50}$ and $D_{84}$ versus step tread $D_{50}$ and $D_{84}$. *Keulegan* [1938] ($D_{50}$) RMSE = 0.012; *Keulegan* [1938] ($D_{84}$) RMSE = 0.018; *Parker and Peterson* [1980] ($D_{84}$) RMSE = 0.06; *Bathurst* [2002] ($D_{84}$) RMSE = 0.115. ESL4 is the largest source of error in each equation.

step type in the reach. Figure 6 shows boxplots using the $ff_{\text{grain}}$ equation with the minimum values for the *Keulegan* [1938] equation using $D_{50}$ and the maximum values using *Parker and Peterson* [1980] and *Bathurst* [2002]. The *Keulegan* [1938] equations (using both reach average and step tread values for $D_{50}$ and $D_{84}$) indicate that reaches with mixed boulder and wood steps have a higher grain resistance than reaches with only boulder, only wood, or no steps. Both the *Bathurst* [2002] and *Parker and Peterson* [1980] equations show no significant difference based on step type. The difference in $ff_{\text{grain}}$ based on the dominant step type may be related to specific characteristics such as the size of the step, which is related to whether the step includes wood or boulders (Figure 7). Steps that are a mixture of wood and boulders tend to have a larger drop height, step height, pool depth, and step width.

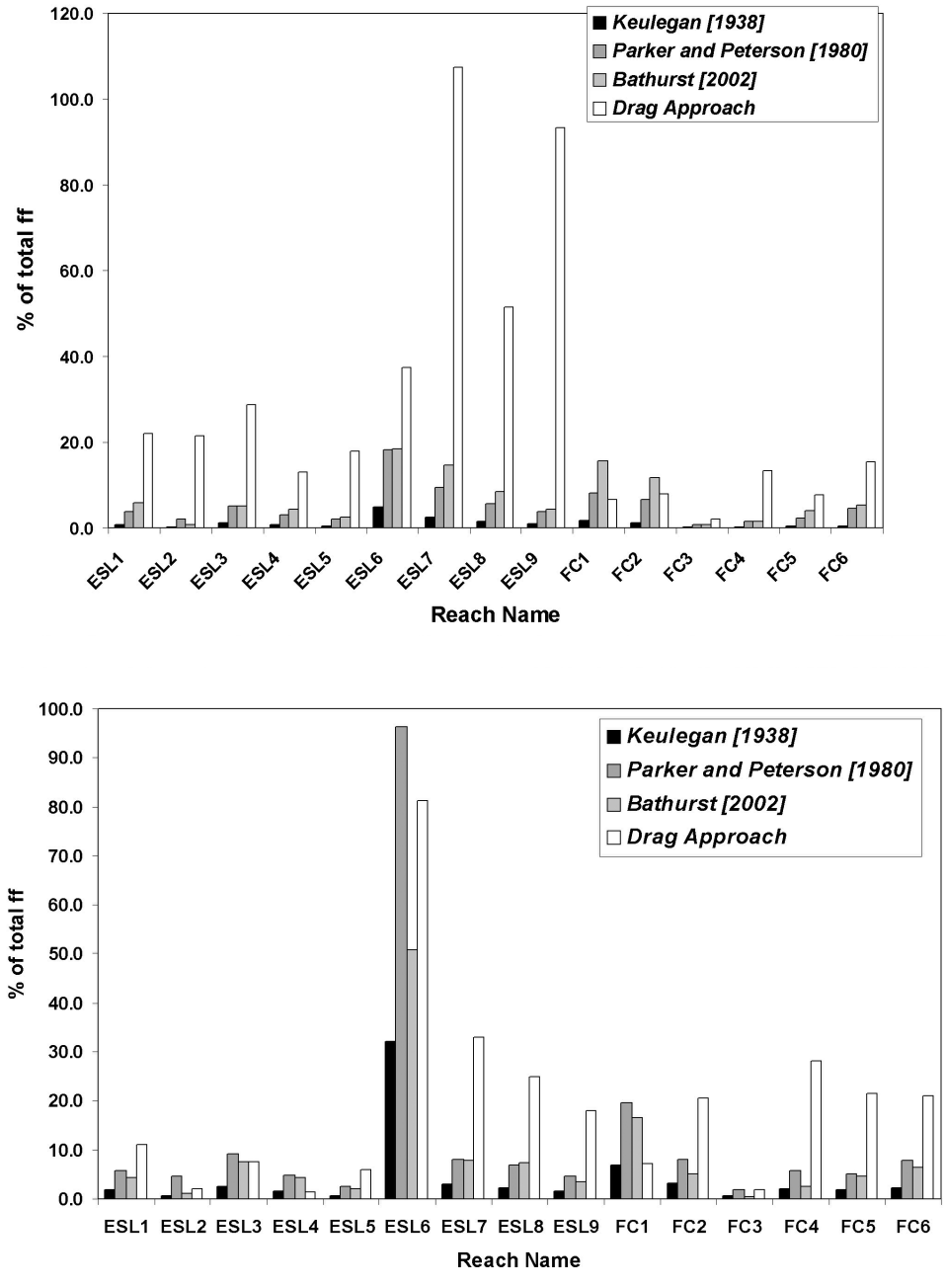


**Figure 5.** Percent contribution of each grain resistance equation of total resistance. (top) August 2007 (low) flows and (bottom) June 2008 (high) flows.

[51] The values of $ff_{grain}$ were also evaluated by flow period and channel type (Figure 6). All the equations, including $ff_{drag}$, showed significantly higher values of $ff_{grain}$ in August 2007 versus June 2008. The drag force approach indicated significantly higher values of $ff_{grain}$ for reaches with mixed step types versus boulder step types in both August 2007 and June 2008. All equations, except $ff_{drag}$, indicated that the values of $ff_{grain}$ are significantly higher in cascade reaches versus step-pool and plane-bed reaches, probably because cascade reaches tend to be on steeper slopes with smaller values of $R/D_{84}$ (between 0.5 and 1.7).

[52] In summary, estimates of percent contribution of grain resistance to $ff_{total}$ are quite sensitive to the equation used, ranging in one channel reach from 32% to 96% at high flows and in another reach from 3% to 15% at low flows (Figure 5). At high flows the *Parker and Peterson* [1980] equation consistently produces the highest estimates and the *Keulegan* [1938] equation consistently produces the lowest estimates of $ff_{grain}$. At low flows the *Bathurst* [2002] equation or drag approach produce the highest estimates and the *Keulegan* [1938] equation produces the lowest estimates of $ff_{grain}$, indicating, as has been previously suggested by *Millar* [1999], that the *Keulegan* [1938] serves as a lower bound for grain resistance. Alternatively, $ff_{grain}$ calculated with the *Bathurst* [2002] equation may better represent a lower bound for total resistance at low flows.

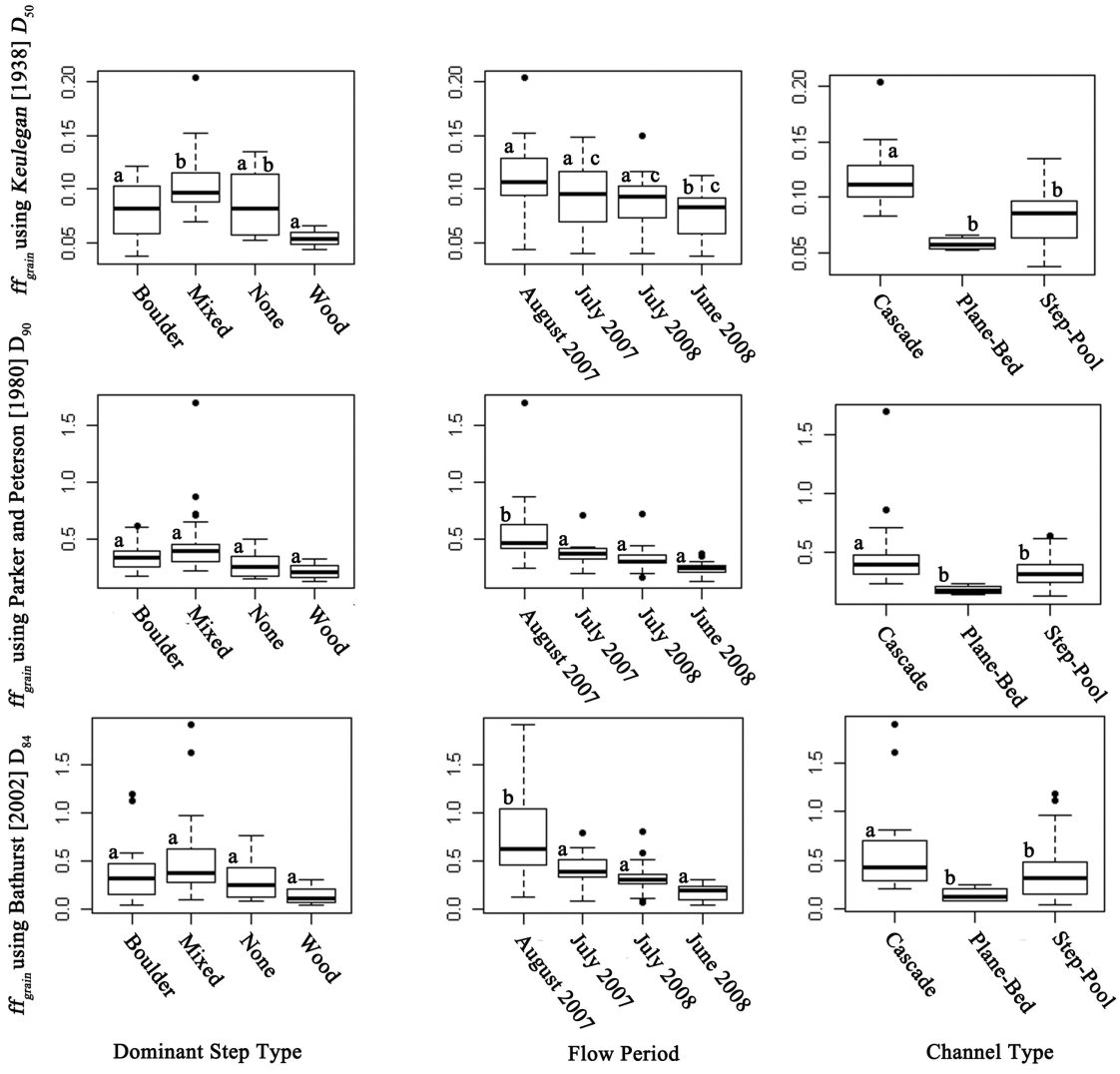


**Figure 6.** Boxplot of grain resistance equations against step type, flow period, and channel type. Step categories: boulder = reaches with only boulder steps, mixed = reaches with both wood and boulder steps, none = reaches with no steps (only ESL6 and ESL7), wood = reaches with only wood steps. Letters a, b, and c show which means are significantly different from each other based on Tukey HSD test in an ANOVA.

[53] The major limitation for calculating grain resistance is that because there is no absolute or widely accepted measure against which to compare varying methods of estimation, it is difficult to evaluate which equation provides the most accurate estimate of the actual value of $ff_{\text{grain}}$. *David* [2011] discusses using the boulder concentration ($\Gamma$) to interpret how well the equations evaluated here represent the grain resistance at both low and high flows. All four equations are significantly related to boulder concentration at high flows, but only the *Keulegan* [1938] equation using both $D_{50}$ and $D_{84}$ is significantly related at low flows. Therefore the *Keulegan* [1938] equation may have a significant association with boulder concentration, but nevertheless lacks fidelity to the physical processes when velocity profiles are not logarithmic and roughness is intermediate and large scale. The *Keulegan* [1938] most likely represents what $ff_{\text{grain}}$ would be if the same grain sizes were placed on a plane-bed channel with an appropriate partial depth and a logarithmic velocity profile. The interactions between $ff_{\text{grain}}$ and other types of resistance, such as ponding from steps, can cause drastic changes in $ff_{\text{grain}}$ from that idealized value.

### 4.2. Wood Resistance ($ff_{\text{wood}}$)

[54] Wood resistance was calculated using the *Shields and Gippel* [1995] approach. There are many potential sources of error in this approach, including the measurement of $X$ (distance between logs), calculation of $C_D^{\text{app}}$, and determination of which pieces constitute significant in-channel wood. The values of $ff_{\text{wood}}$ ranged between 0.01 and 4.43, making up anywhere from 0% to 87% of the $ff_{\text{total}}$ in individual reaches. Although *David et al.* [2010a] found that the wood density using individual logs ($(\sum$ surface area of individual logs)/reach surface area) was not significantly related to $ff_{\text{total}}$, wood is significantly related to $ff_{\text{total}}$ once the wood in steps is included as part of the wood density.

**Table 3.** Regression for $ff_{total}$ Versus $ff_{grain}$[a]

| | *Keulegan* [1938] ($D_{50}$) | *Keulegan* [1938] (Tread $D_{50}$) | *Keulegan* [1938] ($D_{84}$) | *Keulegan* [1938] (Tread $D_{84}$) | *Parker and Peterson* [1980] ($D_{90}$) | *Parker and Peterson* [1980] (Tread $D_{90}$) | *Bathurst* [2002] ($D_{84}$) | *Bathurst* [2002] (Tread $D_{84}$) |
|---|---|---|---|---|---|---|---|---|
| Intercept | 1.92[b] | 1.69[b] | 1.24[c] | 1.88[b] | 0.94[c] | 1.66[b] | 2.49[b] | 2.59[b] |
| $ff_{grain}$ | 16.25[b] | 18.80[b] | 11.25[b] | 9.35[b] | 5.28[b] | 3.92[b] | 1.65[b] | 1.50[b] |
| Aug 2007 | 0.00 | 0.00 | 0.00 | 0.00 | 0.00 | 0.00 | 0.00 | 0.00 |
| Jul 2007 | −0.63 | −0.58 | −0.37 | −0.70[c] | −0.04 | −0.26 | −0.30 | −0.37 |
| Jul 2008 | −0.43 | −0.59 | −0.13 | −0.66 | 0.06 | −0.18 | −0.07 | −0.13 |
| Jun 2008 | −1.21[b] | −1.16[b] | −0.79[c] | −1.19[b] | −0.24[c] | −0.64 | −0.81 | −0.90[c] |
| $R^2$ | 0.39 | 0.46 | 42 | 0.42 | 0.53 | 0.43 | 0.39 | 0.38 |
| adj-$R^2$ | 0.34 | 0.42 | 0.37 | 0.37 | 0.49 | 0.39 | 0.34 | 0.33 |
| *p*-value | <0.001 | <0.001 | <0.001 | <0.001 | <0.001 | <0.001 | <0.001 | <0.001 |

[a]Regressed against $\sqrt{(ff_{total})}$ to meet normality assumptions ($df = 53$). FC3 Jul 2008 was an outlier and removed from regression. Additionally, FC3 August 2007 and FC6 August 2007 were found to be outliers for the *Parker and Peterson* [1980] equation and removed from those regressions. *Parker and Peterson* [1980] = 51 *df*.
[b]Here $a = 0.05$.
[c]Here $a = 0.10$.

Therefore, an additive drag approach may be overestimating the influence of individual logs that are not part of steps on total flow resistance. In some cases, inclusion of all pieces of wood caused the value of $ff_{wood}$ to be more than double the measured value of $ff_{total}$.

[55] Complexly shaped wood pieces also created uncertainty. ESL5 had a log that was primarily a bridge with branches hanging down into the flow. Branches increase the surface area of a log, but also create more flow separation and turbulence [*Hygelund and Manga*, 2003]. Hence the area increases but the drag force does not, so that the apparent drag coefficient decreases. Field observations reveal that the log in ESL5 affects the velocity and depth near the bank, but the *Shields and Gippel* [1995] equation does not provide a way of accurately quantifying that effect. This problem was observed in many reaches, particularly when logs contained branches and were not necessarily in the thalweg, but were obviously responsible for creating flow separation and backwaters.

[56] There are many potential sources of error when using the drag force approach for calculating $ff_{wood}$, as discussed at length in *David* [2011]. First, wood in steps was considered part of the step form and thus was not considered as part of $ff_{wood}$. Second, each parameter in equations (13) through (17) has associated potential error based on measurement errors as well as estimating unknowns such as the drag coefficient ($C_D$). The drag coefficient ($C_D$) and empirically derived values for $a$ and $b$ are likely the largest source of error in calculating $ff_{wood}$. A sensitivity analysis for calculating $ff_{wood}$ for two step-pool reaches using a reasonable range of drag coefficients for each log indicates that the larger the value of $ff_{wood}$, the greater the error associated with choosing a value of $C_D$.

[57] The distance between objects is another potentially substantial source of error. The value $X$ in equation (17) is commonly the distance between logs, but in the case of these high-gradient mountain streams, logs are not the only objects significantly affecting the flow and creating wakes that affect the drag around individual logs. Therefore we evaluated $X$ as the distance between objects producing appreciable wakes, which included steps and large boulders that were observed to help in the formation of wave drag.

### 4.3. Step Resistance ($ff_{step}$) and $ff_{spill}$

[58] Steps likely contribute the greatest proportion of resistance in step-pool channels from both spill and form resistance [*Curran and Wohl*, 2003; *Wilcox et al.*, 2006]. Form resistance relates to energy losses from circulation in

**Table 4.** Each Grain Resistance Equation Versus $ff_{drag}$[a]

| | *Keulegan* [1938] ($D_{50}$) $\sqrt{(ff_{drag})}$ | *Keulegan* [1938] (Tread $D_{50}$) $\sqrt{(ff_{drag})}$ | *Keulegan* [1938] ($D_{84}$) | *Keulegan* [1938] (Tread $D_{84}$) | *Parker and Peterson* [1980] ($D_{90}$) | *Parker and Peterson* [1980] (Tread $D_{90}$) | *Bathurst* [2002] ($D_{84}$) | *Bathurst* [2002] (Tread $D_{84}$) |
|---|---|---|---|---|---|---|---|---|
| | | | | *June 2008* | | | | |
| Intercept | −0.05 | 0.08 | −0.55 | −0.46 | −0.40 | 0.36 | 0.19 | 0.1 |
| $ff_{grain}$ | 9.34* | 7.82** | 8.15** | 7.88** | 4.13** | 1.69 | 1.99 | 3.15** |
| $R^2$ | 0.42 | 0.34 | 0.3 | 0.31 | 0.37 | 0.2 | 0.19 | 0.4 |
| adj-$R^2$ | 0.37 | 0.29 | 0.25 | 0.26 | 0.31 | 0.14 | 0.13 | 0.35 |
| *p*-value | 0.009 | 0.02 | 0.03 | 0.04 | 0.02 | 0.11 | 0.11 | 0.02 |
| | | | | *August 2007* | | | | |
| Intercept | 0.92* | 0.75 | −0.55 | 2.64 | 1.56 | 2.42 | 2.90* | 3.09** |
| $ff_{grain}$ | 6.17 | 7.92** | 8.15** | 0.75 | 2.47 | 0.76 | −0.14 | −0.38 |
| $R^2$ | 0.16 | 0.27 | 0.3 | 0.0006 | 0.05 | 0.006 | 0.001 | 0.008 |
| adj-$R^2$ | 0.09 | 0.21 | 0.25 | −0.09 | −0.03 | −0.08 | −0.09 | −0.08 |
| *p*-value | 0.16 | 0.06 | 0.03 | 0.94 | 0.45 | 0.81 | 0.92 | 0.77 |

[a]ESL3 and ESL4 outliers for *Bathurst* [2002] (tread). ESL4 removed as outlier in *Keulegan* [1938] (ST). In every regression ESL3, ESL4, and FC4 seem to have higher leverage than other reaches. For August 2007 regressions ESL9 and FC6 were outliers.

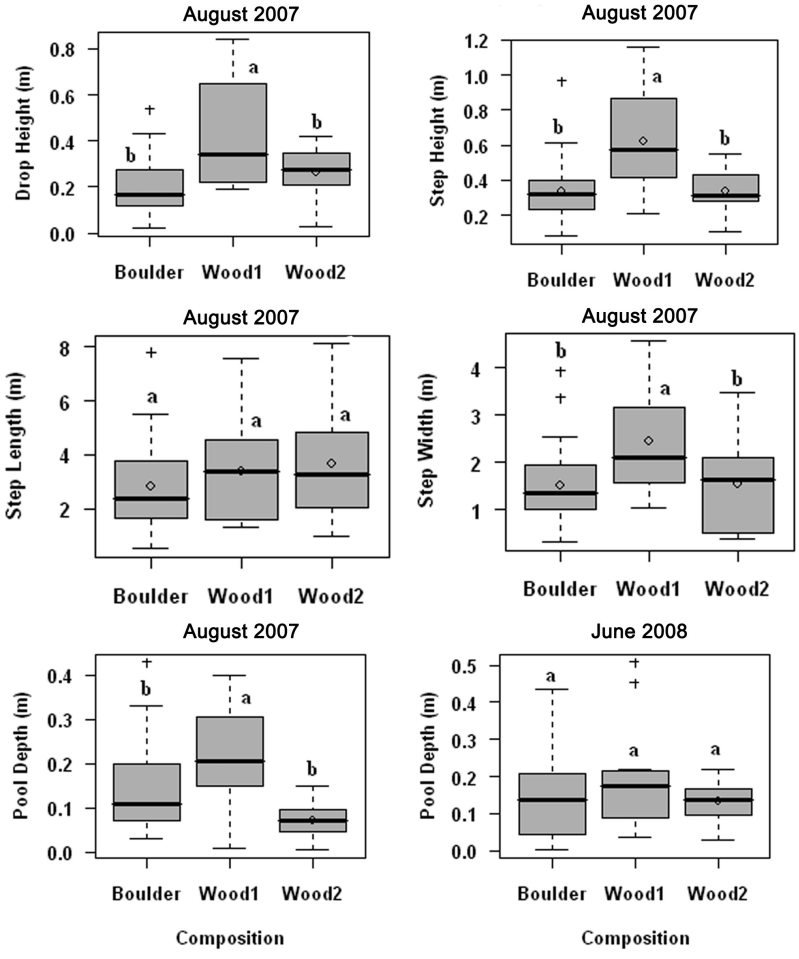


**Figure 7.** Boxplot of step dimensions for every individual step in every reach based on step composition. Boulder, steps only made up of large grains; wood1, steps made up of a keystone boulder and wood; wood2, steps only made up of wood. Letters a and b indicate which means are significantly different from each other using a Tukey HSD test in an ANOVA.

the pools, but as steps become submerged, the step shape can also contribute to form losses. We calculated form resistance around steps using a drag force approach. Because $C_D$ is unknown, we performed a sensitivity analysis for one cascade and two step-pool reaches (Figure 8). The percent contribution of $ff_{step}$ to $ff_{total}$ can vary from 1% to 63% within a reach, depending on the values of the drag coefficient. The more conservative lower values of $ff_{step}$, using the smallest values of $C_D$, were compared to the other components because the larger values sometimes exceeded $ff_{total}$ when added together with the other components of resistance. The contribution of $ff_{step}$ to $ff_{total}$ tended to be highest during the high flows, since these were the times that the steps had either submerged or skimming flow over the step. *Smart et al.* [2002] argued that bedforms are not significant in streams where other bed elements are on the same order of magnitude as the flow depth, but our results suggest that the adverse pressure gradient around bedforms may become increasingly important as flow increases despite the presence of other bed elements on the same order of magnitude as flow depth. At lower discharges, $ff_{spill}$ may dominate with higher drop heights and smaller pools.

### 4.4. Overview of Total and Component Resistance

[59] Figure 9 shows the results of the additive partitioning of $ff_{grain}$, $ff_{wood}$, $ff_{step}$, and $ff_{spill}$. The *Keulegan* [1938] equation was used to calculate grain resistance using $D_{50}$ since this equation seemed to give a lower bound for $ff_{grain}$. The same equation was used for low and high flows to avoid introducing another source of variability. The wood and step components were calculated using the drag approach outlined above. Spill resistance was estimated as the component remaining after all other components were subtracted from $ff_{total}$, although the term spill also incorporates any other unmeasured form of resistance such as bank resistance. Each component of resistance most likely interacts with other components, so bank effects may also be included in the step, wood, or grain component. In the additive approach, some of the added values of total resistance from $ff_{grain} + ff_{wood} + ff_{step}$ exceeded $ff_{total}$, therefore these reaches are not shown to contain any $ff_{spill}$ because of the overestimate of one or all of the other components. Grain resistance contributed the smallest amount for all the reaches, including the plane-bed reach. Wood resistance contributed a large proportion of the total resistance at high

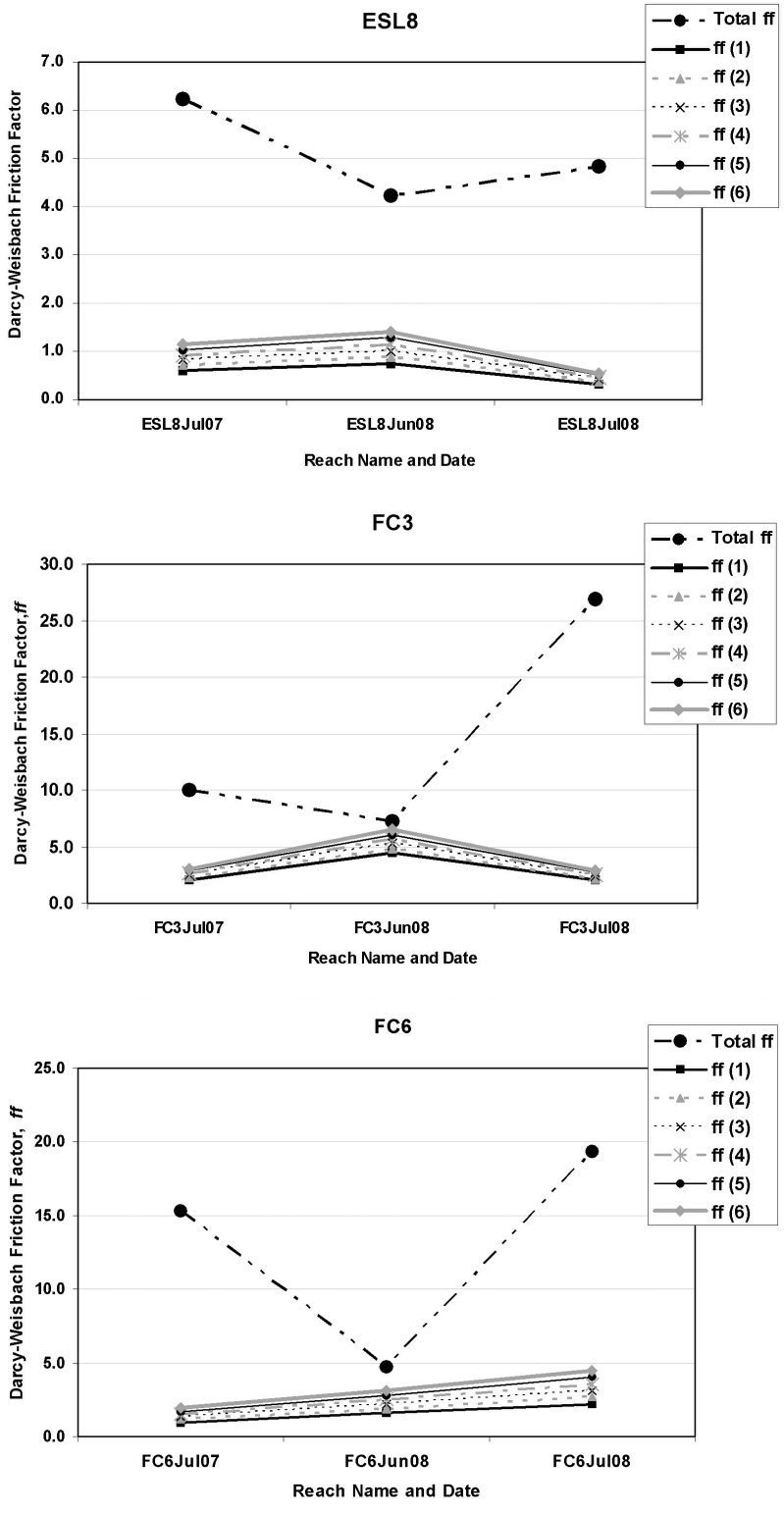


**Figure 8.** Example of sensitivity analysis for $ff_{step}$. Each number in the key (1–6) indicates that a different drag coefficient was used for each iteration. 1 is related to the smallest values of $C_D$ used and 6 are the maximum values. Depending on the reach, the larger drag coefficients could double the percent contribution of $ff_{step}$: ESL8 ranged from 28% to 52% at high flows, FC3 went from 61% to 89% at high flows, and FC6 goes from 33% to 66% at high flows.

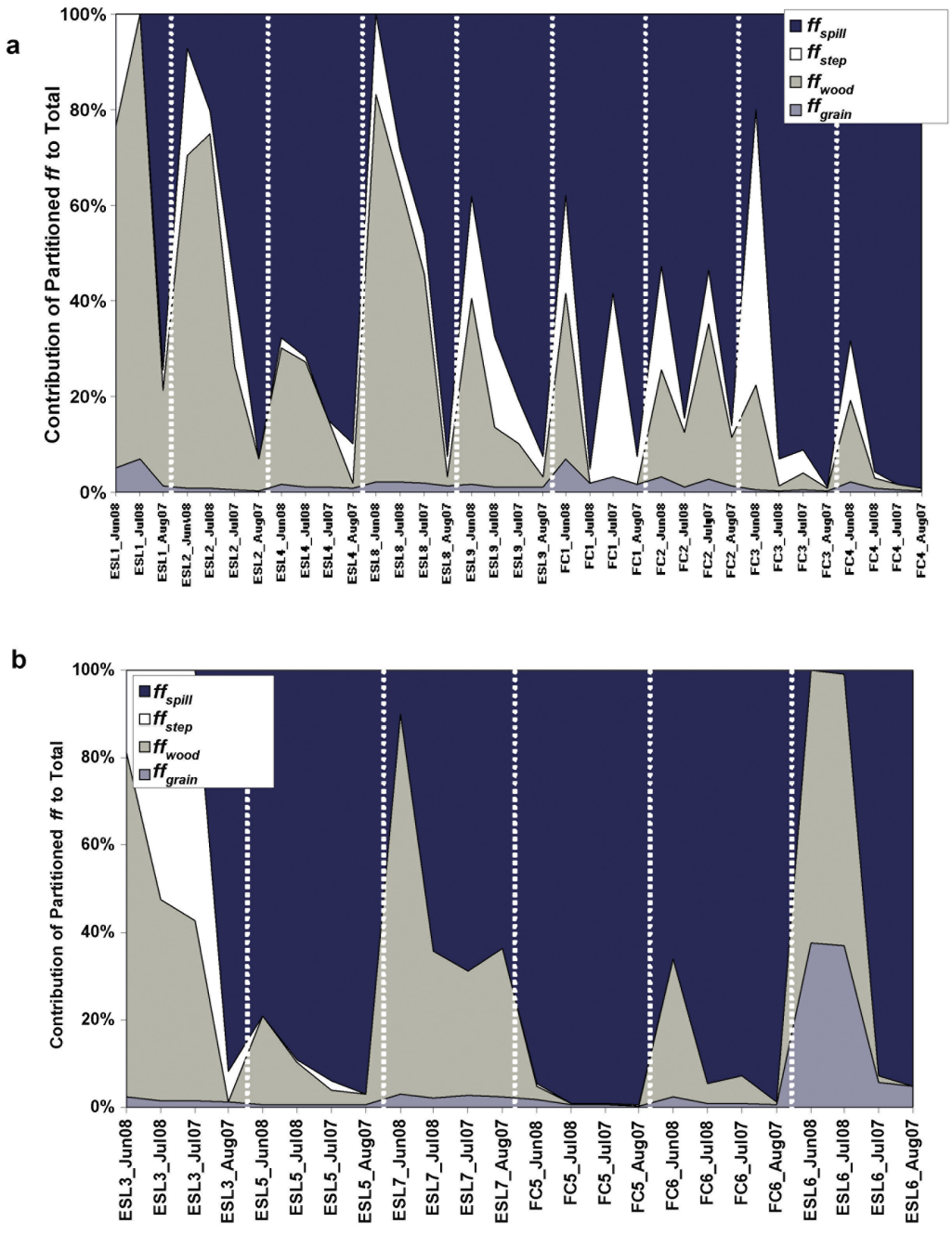


**Figure 9.** Contribution of partitioned friction factor to total: (a) step-pool reaches and (b) cascade reaches. Dotted white lines indicate division between reaches. The $ff_{spill}$ were made to be zero where negative values existed, because additive components exceeded the value of $ff_{total}$. Figure shows partitioned values for each reach over each flow period.

flows and progressively smaller amounts as discharge decreased and logs were no longer submerged. Conversely, the contributions of $ff_{spill}$ increased progressively as discharge decreased (Figure 10). Step resistance is related to discharge in that it was calculated only for steps that met a specific submergence criterion. Spill and $ff_{step}$ contributed the greatest amount to total resistance at all flows for a majority of the reaches, except for four reaches during high flows. Two of these reaches do not include any steps and all four have a large wood component at high flows.

[60] The cascade reaches had a smaller contribution from $ff_{step}$ to $ff_{total}$, therefore the unmeasured component ($ff_{spill}$) contributed the most in these reaches. However, the unmeasured component of spill resistance was not always the largest proportion of the total resistance in every reach (Figures 9). Boxplots of the percent contribution of each component of resistance for cascade versus step-pool reaches (Figure 11) indicate that the only significant difference in the percent contribution is from $ff_{step}$ during high flows. There are significantly higher values of $ff_{grain}$ in the

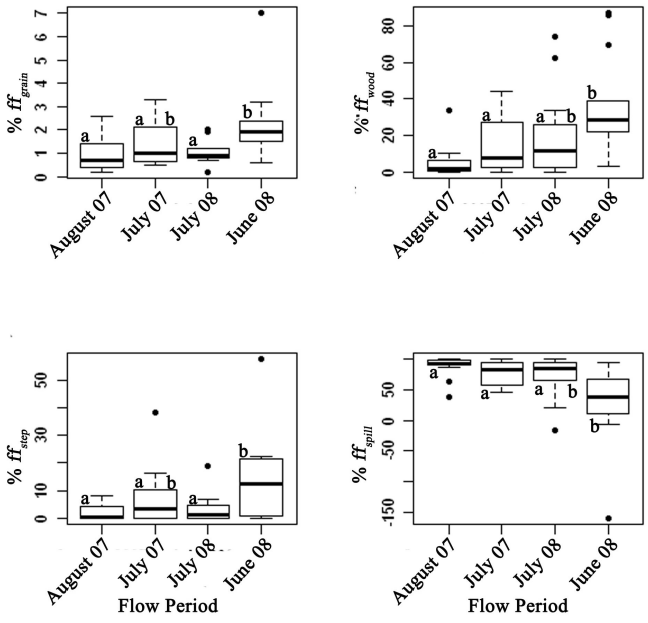


**Figure 10.** Boxplots of percentage contribution of each component of resistance for each flow period. ESL3 is excluded from the boxplots. Boxes with the same letter (a, b, c) have means similar at $\alpha = 0.05$ $= 0.05$.

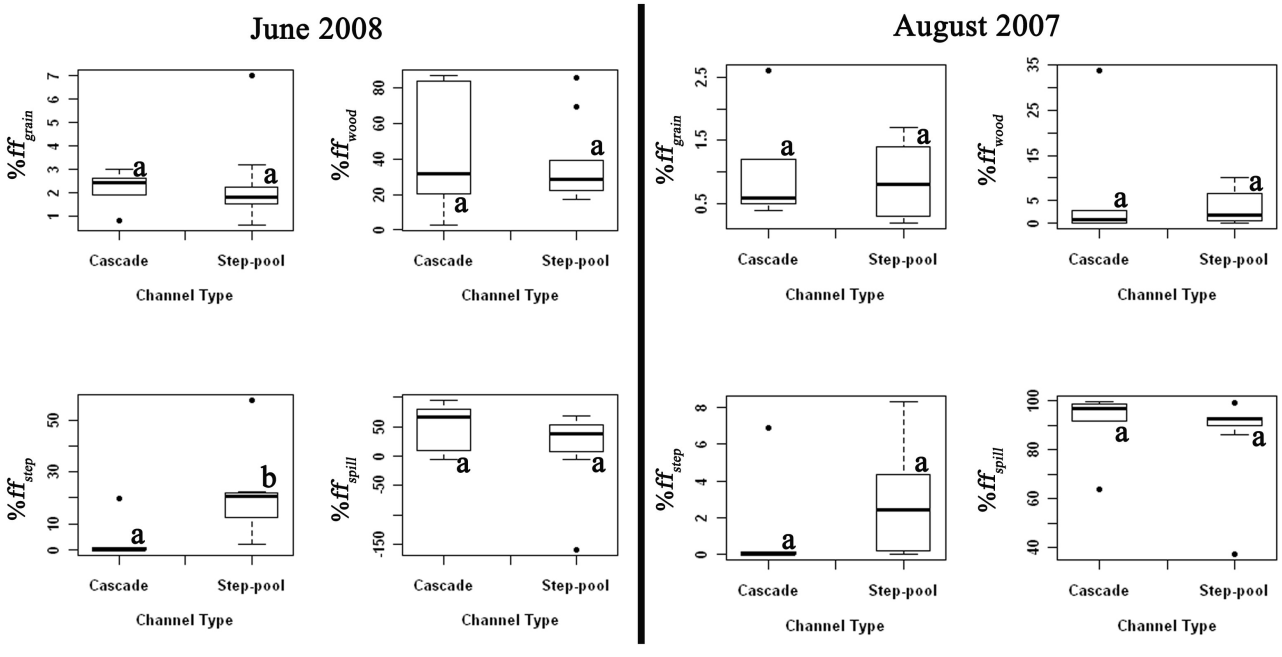


**Figure 11.** Boxplots showing the percent of total resistance related to grain, wood, step, and spill for each channel type. The % $ff_{\text{step}}$ has significantly different means for cascade versus step-pool reaches. Letters a and b indicate significantly different means using Tukey HSD test in an ANOVA ($\alpha = 0.05$).

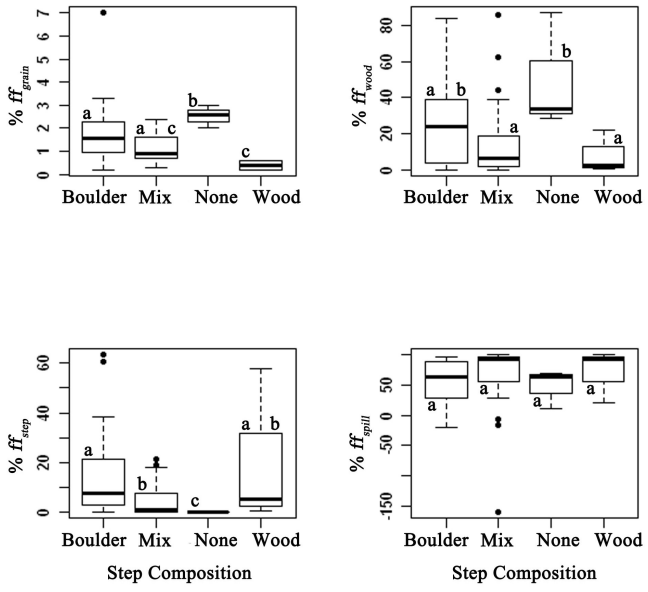


**Figure 12.** Boxplot of percent contribution of each partitioned component according to dominant step composition within the reach. Boulder, reach dominated by boulder steps; mix, reach has a combination of wood and boulder steps; none, reach has no steps (only ESL7); wood, reach only has wood steps. ESL6 excluded from these groupings, but inclusion only increases difference between none and other categories. ESL3 is excluded because of the large deviation from $ff_{total}$ due to the large number calculated for $ff_{step}$. Boxes with the same letter (a, b, c) have means similar at $\alpha = 0.05$.

cascade reaches (Figure 6), but overall the $\%ff_{grain}$ is not different for these reaches versus the step-pool reaches. There is more variability in $\%ff_{grain}$ in the step-pool reaches during low flows and greater variability in the $\%ff_{wood}$ for cascade reaches during high flows, despite a lack of significant differences between the means (Figure 11). The contribution from each component of resistance also varied with the step composition (Figure 12). The percent contribution of $ff_{grain}$ and $ff_{wood}$ was significantly higher for reaches without any steps than for the reaches with steps. The reaches dominated by boulder steps had a higher $\%ff_{grain}$ than reaches with only wood steps.

[61] On average the major contributions toward $ff_{total}$ are from $ff_{wood}$ and $ff_{spill}$. As noted in the flume by *Wilcox et al.* [2006], the contribution from $ff_{spill}$ is reduced during high flows (Figure 10). Otherwise the contribution of each component ($ff_{wood}$, $ff_{step}$, $ff_{grain}$) is significantly larger during high flows.

## 5. Discussion

[62] Ability to quantify the effects of each component of total resistance remains limited by the available methods. The methods discussed here assume that each component of resistance affects the total in isolation and that the individual components can be added to calculate $ff_{total}$ [*Wilcox et al.*, 2006]. The unmeasured component remained the largest in most of our study reaches, particularly at lower flows. The unmeasured component is assumed to be related to $ff_{spill}$, although it could also be related to bank resistance, which was neglected in this study. The results suggest that the current additive approach is not appropriate and that the unmeasured component tends to be large because individual sources of resistance interact in complex fashions that effectively alter the resistance associated with any individual component relative to the resistance of that component in isolation. Yet the additive approach could be greatly improved if the error associated with many of the variables (e.g., $C_D^{app}$) used to calculate $ff_{grain}$, $ff_{wood}$, or $ff_{step}$ was reduced.

### 5.1. Methods for Calculating $ff_{grain}$ and Associated Limitations

[63] Each of the current methods used to calculate $ff_{grain}$ may be appropriate for high flows, where the majority of the grains are submerged, but appear to completely underestimate the contribution of $ff_{grain}$ during low flows. Low flows in the study reaches are distinct from other stages by having a majority of the larger bed material only partially inundated and relative roughness $R/D_{84} \leq 1$. Although *Ferguson* [2007] defined shallow flows as $R/D_{84} \leq 4$, the reaches in this study are all below 4 at high and low flows. Divisions for $R/D_{84}$ should also vary based on gradient [*David et al.*, 2010a] such that, for gradients closer to 0.10, the limit for shallow flows might lie closer to 1.5–2.0.

[64] During low flows the values of grain resistance increase but the contributions toward $ff_{total}$ decrease. Each of these equations is possibly underestimating $ff_{grain}$ at low flows because of the inherent unsuitability of using an approach that assumes a logarithmic velocity profile [*Wiberg and Smith*, 1991; *Katul et al.*, 2002]. Near-bed velocities remain low up to a grain size of $D_{16}$ and increase rapidly when flow is above the range of $D_{50}$ and $D_{84}$ [*Wiberg and Smith*, 1991].

[65] Despite these differences, we still found $D_{84}$ to be a representative length scale and the relative roughness can be related to the nondimensionalized velocity ($\bar{v}/u^*$) by a

log linear curve. Summing the contribution of each large grain over the entire reach using the drag force approach indicates that the contribution from $ff_{grain}$ could be much larger than calculated by these equations (Figure 5). *Wilcox et al.* [2006] also found that both the *Bathurst* [2002] and *Parker and Peterson* [1980] equations consistently underestimated grain resistance.

[66] The *Keulegan* [1938] equation, using both $D_{50}$ and $D_{84}$, consistently underestimated $ff_{grain}$, which was determined by evaluating the contribution of $\%ff_{grain}$ to $ff_{total}$ in the plane-bed reach. At the lowest flow, when the other sources of resistance are reduced by the lack of in-channel wood and reduced bank resistance, the $\%ff_{grain}$ was 4.9% (Figure 5). In contrast, the drag approach indicates that $ff_{grain}$ makes up 33% of $ff_{total}$. The drag approach is probably also underestimating $ff_{grain}$ since only a few larger grains were exposed at low enough flows to be surveyed in this reach using the LiDAR pointclouds. Smaller grain sizes probably start to affect the flow as stage decreases, so these should be accounted for in a drag approach. On the other hand, the *Keulegan* [1938] equation had a more significant relationship with $ff_{total}$ and $ff_{drag}$ at all flows, particularly when using the step tread $D_{50}$, despite the assumed lack of a logarithmic velocity profile (Tables 3 and 4). The relationship between the *Keulegan* [1938] and $ff_{drag}$ indicates that even with the use of a smaller grain size such as $D_{50}$, the *Keulegan* [1938] still captures a portion of the form drag component around the grains.

[67] Flow accelerates on the step tread as it approaches the step lip [*Wohl and Thompson*, 2000; *Wilcox and Wohl*, 2007]. An interaction of processes is evident here; a larger step causes a larger backwater area, allowing deposition of finer material and greater difference in flow acceleration between low and high flows. Reaches with large wood steps have finer material and larger rates of change of velocity with discharge [*David et al.*, 2010b]. Both grain resistance and ponding are significant at low flows and can drastically reduce velocity. The effect of grain resistance at those lower stages is not easily quantified by equations based on the law of the wall and a large characteristic grain diameter. There are two levels of resistance related to the presence of grains in the flow: (1) water flowing around large boulders creating areas of flow separation and reattachment and (2) water flowing over smaller grains creating small surface waves and hydraulic jumps, which can also be defined as spill resistance over the grains. Since the spill resistance is caused by the presence of grains, we still define it here as grain resistance. Additionally, both levels include viscous skin friction around the grain. The first type of grain resistance may be best represented by a large characteristic grain size $D_{90}$. *Parker and Peterson*'s [1980] equation was significantly related to boulder concentration at high flows, indicating that a larger representative grain size captures the combined form drag and skin friction around individual boulders. The second grain resistance may be best characterized by $D_{50}$ since the *Keulegan* [1938] equation was significantly related to both the values determined from the drag force equation and the boulder concentration. The median grain size is more likely to remain submerged at lower flows and can better represent a lower bound of $ff_{grain}$.

[68] Although sorting was not significantly related to $ff_{total}$ [*David et al.*, 2010a], the sorting may have a significant effect on the values of $ff_{grain}$ at low flow. The larger boulders and smaller grains influence the overall hydraulics in a very different way at low flows. Most studies focus on finding one representative grain size and determining a multiplier for that grain size to fit it into some type of *Keulegan* [1938] relation [*Hey*, 1979; *Reid and Hickin*, 2008]. In mountain streams it is possible that two values of $ff_{grain}$ should be estimated from two different representative grain sizes (e.g., $D_{50}$ and $D_{90}$) and two different equations for low and high flows, as suggested by *Ferguson* [2007].

[69] Based on the analyses presented above, we recommend using the *Parker and Peterson* [1980] approach to calculate $ff_{grain}$ in steep streams during bank-filling flows. This approach is the least sensitive to morphological location of the pebble count because it uses such a large characteristic grain size, but it takes a much larger sample size pebble count to estimate $D_{90}$ with the same accuracy as $D_{50}$. Also, the values of $ff_{grain}$ for the *Parker and Peterson* [1980] equation were most significantly related to the boulder concentration at high discharges. The *Keulegan* [1938] equation might be the better approach, despite being dependent on a logarithmic velocity profile for determining a base level of $ff_{grain}$ at both low and high flows. At low flows the values of relative submergence ($R/D_{84}$) approach zero, with values ranging between 0.52 and 2.18. Using a smaller characteristic grain size at low flows will improve the validity of these equations. Also, the predictions at low flow may be improved by developing an equation that uses two characteristic grain sizes. One grain size should represent the larger bed elements that are only partially inundated and cause the flow to move around rather than over the objects. The second should represent the grains that are submerged but still cause distortions in the flow field. The difference between high and low flows is related to the relative submergence *Fr* and *Re.* The combined approach may be best utilized by adding the drag force component around boulders as large as the $D_{90}$. The *Keulegan* [1938] equation can be used for calculating the grain resistance related to skin friction and form drag along smaller, submerged grains. In step-pool reaches the step tread grain size should be used to account only for grain resistance. Grains that are part of the actual step should be included as the $ff_{spill}$ and $ff_{step}$ components.

### 5.2. Methods for Calculating $ff_{wood}$ and Associated Limitations

[70] The *Shields and Gippel* [1995] approach of calculating $ff_{wood}$ commonly overestimated the total value of $ff_{wood}$. Although the values of the $C_D$ were well within the range found by *Gippel et al.* [1992], there is still some question as to appropriate values. The blockage ratio exceeded the range tested by *Gippel et al.* [1992], suggesting that the empirically derived values of $a$ and $b$ used in equation (13) may not be correct for these streams. In other studies, $C_D$ has ranged from 1.2 [*Manga and Kirchner*, 2000; *Hygelund and Manga*, 2003] to 6.0 [*Curran and Wohl*, 2003], but values over 1.0 commonly led to values of $ff_{wood}$ that exceeded $ff_{total}$.

[71] There are a number of problems with this approach revealed in this analysis. First, the *Shields and Gippel* [1995] approach assumes that $ff_{wood}$ can be calculated for each individual log and then added to estimate total $ff_{wood}$. Second, the drag force approach does not account well for logs with branches or for the position of the log in the water

column. Third, *Hygelund and Manga* [2003] found that $C_D^{app}$ scaled with depth ratio (a measure of the relative depth of the log) more than with blockage ratio. Fourth, the drag force approach did not do well in capturing the wake effect from upstream objects, which may reduce the effect of the log downstream. Fifth, the distance between objects $X$ is difficult to determine since there is no standardized approach for evaluating $X$. Also, the more closely spaced objects were, the higher the value of $ff_{wood}$. This approach assumes that the drag force is applied over a short distance, but does not account for the effect of the wake interference from the upstream object, which could cause reduced drag on the downstream object.

### 5.3. Methods for Calculating $ff_{step}$ and Associated Limitations

[72] Researchers have found that step height and length are significantly related to $ff_{total}$ in step-pool channels [*Abrahams et al.*, 1995; *Maxwell and Papanicolaou*, 2001], but both $H_s$ and $L_s$ are assumed to only relate to $ff_{spill}$. *Smart et al.* [2002] argue that the form drag around bedforms is not as significant as form drag around individual particles, since the individual particles are of the same size as the flow depth. This may be true, depending on the size of the bed elements relative to the flow depth, but it does not explain the paucity of data on evaluating the form drag around the step and pool bedforms rather than just the spill resistance. Random arrangements of boulders dissipate much less energy than boulders arranged in rows [*Pagliara and Chiavaccini*, 2006]. The results of an analysis of the drag force around the step bedforms indicate that as the bed form becomes increasingly submerged and the flow approaches a skimming flow, a wake can develop around the bed form, increasing the form resistance at higher flows (Figure 2). As grains on step treads and even in the pools protrude further into the flow with decreasing stage, the effect of the bedforms may disappear relative to the effect of the grains and from nappe flow increasing spill resistance over the step. The conflicting interpretations from previous studies suggest that systematic evaluations of form drag around bedforms in relation to varying stage are needed, particularly when steps are more closely spaced together.

[73] The wood jams that make up a number of steps create added drag depending on the porosity of the jam. Increased porosity leads to increased flow through the jam and increased shear stress applied to the bed downstream from the jam [*Manners et al.*, 2007]. The jam that *Manners et al.* [2007] studied did not create a step, as jams tend to in high-gradient channels, but further work is needed on how flow through and over steps varies the drag force and contribution of the step to $ff_{total}$. *Manners et al.* [2007] also suggested that the jam geometry is inextricably linked with the drag coefficient, meaning that a combined value needs to be calculated for each jam. Since local velocities were not measured, this was not attempted in these reaches, but may be important to consider in future work.

## 6. Conclusion

[74] The method of additive partitioning does not accurately predict flow resistance for high-gradient step-pool and cascade streams. Problems were identified even in the calculation of $ff_{wood}$ in the smaller and less complicated plane-bed reach. All methods for calculating each component of resistance had many problems and limitations once applied to these steep streams that included large volumes of wood. It was difficult to evaluate which method of calculating $ff_{grain}$ was most accurate, as there is no standard against which to compare the values. The *Parker and Peterson* [1980] equation seemed to better represent $ff_{grain}$ at high flows based on its relationship to boulder concentration at higher flows and the insensitivity of the equation to the morphologic position of the grains. On the other hand, the *Bathurst* [2002] equation is more often preferred because it is based on a power relationship and not a logarithmic relationship and may better represent a lower bound for total resistance in streams with intermediate- and large-scale roughness. No correlation was found between the *Parker and Peterson* [1980] equation and boulder concentration for $ff_{grain}$ from form drag at low flows. The *Keulegan* [1938] equation using both $D_{84}$ and $D_{50}$ had the closest relationship with some of the physical descriptors related to grain resistance, but could still be underestimating the actual values of $ff_{grain}$. The values were always the smallest at both low and high flows, but at low flows the *Keulegan* [1938] equation was significantly related to both boulder concentration and $ff_{grain}$ from the drag approach. The *Keulegan* [1938] equation would therefore be a conservative lower estimate of $ff_{grain}$ at low flows, but more work needs to be done to determine how best to calculate grain resistance when $R/D_{84} \ll 1$.

[75] The lower flow regime may create problems in calculating drag around objects because of the variation in the drag coefficient with $Re < 10^4$. The relative submergence of the step, in relation to nappe, submerged nappe, and skimming flows, may be significant when determining separate contribution from $ff_{step}$ and $ff_{spill}$. During low flows the effect of $ff_{spill}$ just downstream of steps and $ff_{grain}$ on step treads may begin to dominate $ff_{total}$. More work needs to be done to understand how form drag around step bedforms contributes to flow resistance.

[76] The drag method for calculating $ff_{wood}$ was applied to individual logs in the channel, but the large number of variables in which there is uncertainty allows large sources of error. The distance between logs $X$ should be better defined for natural channels where there are other large sources of resistance. Nonetheless, the contribution of $\%ff_{wood}$ toward $ff_{total}$ was higher than expected for many of the reaches based on field observations. The value of $ff_{wood}$ was highly dependent on discharge since at lower flows very few logs were effectively within the flow. Also, values of $C_D$ from low-gradient flumes do not necessarily apply well to wood in high-gradient channels. More work is needed to measure values of $C_D$ in the field. Physically based methods for estimating spill resistance and partitioning of resistance that include the interactions among components are also needed. Flume experiments may be particularly helpful in developing new methods and numerical simulations applicable to high-gradient channels.

[77] **Acknowledgments.** This research was funded by the Hydrologic Sciences Program of the National Science Foundation (EAR 0608918). The USDA Forest Service Rocky Mountain Research Station and field assistants Mark Hussey, Dan Dolan, Alexandra David, Lina Polvi, and

Dan Cadol provided logistical support. We thank two anonymous reviewers and Dieter Rickenmann for their comments, which helped to improve the manuscript. Furthermore, we would like to thank dissertation committee members Daniel Cenderelli and Sandra Ryan-Burkett for their comments and support.

## References

Aberle, J., and G. M. Smart (2003), The influence of roughness structure on flow resistance on steep slopes, *J. Hydraul. Res.*, *41*, 259–269.

Abrahams, A. D., G. Li, and J. F. Atkinson (1995), Step-pool streams: Adjustment to maximum flow resistance, *Water Resour. Res.*, *31*, 2593–2602, doi:10.1029/95WR01957.

Baiamonte, G., and V. Ferro (1997), The influence of roughness geometry and Shields parameter on flow resistance in gravel-bed channels, *Earth Surf. Processes Landforms*, *22*, 759–772.

Bathurst, J. C. (1982), Flow resistance in boulder-bed streams, in *Gravel-bed Rivers*, edited by R. G. Li, J. C. Bathurst, and C. R. Thorne, pp. 443–465, John Wiley, Hoboken, N. J.

Bathurst, J. C. (1985), Flow resistance estimation in mountain rivers, *J. Hydraul. Eng.*, *111*, 625–643.

Bathurst, J. C. (1993), Flow resistance through the channel network, in *Channel Network Hydrology*, edited by K. Beven and M. J. Kirkby, pp. 69–98, John Wiley, New York.

Bathurst, J. C. (2002), At-a-site variation and minimum flow resistance for mountain rivers, *J. Hydrol.*, *269*, 11–26.

Calkins, D., and T. Dunne (1970), A salt tracing method for measuring channel velocities in small mountain streams, *J. Hydrol.*, *11*, 379–392.

Canovaro, F., E. Paris, and L. Solari (2007), Effects of macro-scale bed roughness geometry on flow resistance, *Water Resour. Res.*, *43*, W10414, doi:10.1029/2006WR005727.

Chanson, H. (1994), *Hydraulic Design of Stepped Cascades, Channels, Weirs and Spillways*, 261 pp., Pergamon, Oxford, U. K.

Chanson, H., and L. Toombes (2002), Experimental investigations of air entrainment in transition and skimming flows down a stepped chute, *Can. J. Civ. Eng.*, *29*(1), 145–156.

Chartrand, S. M., and P. J. Whiting (2000), Alluvial architecture in headwater streams with special emphasis on step-pool topography, *Earth Surf. Processes Landforms*, *25*, 583–600.

Church, M., and A. Zimmerman (2007), Form and stability of step-pool channels: Research progress, *Water Resour. Res.*, *43*, W03415, doi:10.1029/2006WR005037.

Comiti, F., A. Andreoli, L. Mao, and M. A. Lenzi (2008), Wood storage in three mountain streams of the Southern Andes and its hydro-morphological effects, *Earth Surf. Processes Landforms*, *33*, 244–262, doi:10.1002/esp.1541.

Comiti, F., D. Cadol, and E. Wohl (2009), Flow regimes, bed morphology, and flow resistance in self-formed step-pool channels, *Water Resour. Res.*, *45*, W12804, doi:10.1029/2010WR009699.

Curran, J. H., and E. E. Wohl (2003), Large woody debris and flow resistance in step-pool channels, Cascade Range, Washington, *Geomorphology*, *51*, 141–157.

David, G. C. L. (2011), Characterizing flow resistance in steep mountain streams, Fraser Experimental Forest, Colorado, Ph.D. dissertation, 350 pp., Colo. State Univ., Fort Collins.

David, G. C. L., E. E. Wohl, S. E. Yochum, and B. P. Bledsoe (2010a), Controls on spatial variations in flow resistance along steep mountain streams, *Water Resour. Res.*, *46*, W03513, doi:10.1029/2009WR008134.

David, G. C. L., E. E. Wohl, S. E. Yochum, and B. P. Bledsoe (2010b), Controls on at-a-station hydraulic geometry relationships in steep headwater streams, *Earth Surf. Processes Landforms*, *35*, 1820–1837, doi:10.1002/esp.2023.

Einstein, H. A., and N. L. Barbarossa (1952), River channel roughness, *Trans. Am. Soc. Civ. Eng.*, *117*, 1121–1146.

Ferguson, R. I. (2007), Flow resistance equations for gravel- and boulder-bed streams, *Water Resour. Res.*, *43*, W05427, doi:10.1029/2006WR005422.

Ferguson, R. I. (2010), Time to abandon the Manning equation?, *Earth Surf. Processes Landforms*, *35*, 1873–1876.

Ferro, V. (2003), Flow resistance in gravel-bed channels with large-scale roughness, *Earth Surf. Processes Landforms*, *28*, 1325–1339, doi:10.1002/esp.589.

Gippel, C. J., I. C. O'Neill, and B. L. Finlayson (1992), *The Hydraulic Basis for Snag Management*, Centre for Environmental Applied Hydrology, Department of Civil and Agricultural Engineering, University of Melbourne, Melbourne, Vic., Australia, 116 p.

Gippel, C. J., B. L. Finlayson, and I. C. O'Neill (1996), Distribution and hydraulic significance of large woody debris in a lowland Australian river, *Hydrobiologia*, *318*, 179–194.

Grant, G. E. (1997), Critical flow constrains flow hydraulics in mobile-bed streams: A new hypothesis, *Water Resour. Res.*, *33*(2), 349–358, doi:10.1029/96WR03134.

Griffiths, G. A. (1989), Form resistance in gravel channels with mobile beds, *J. Hydraul. Eng.*, *115*, 340–355.

Hey, R. D. (1979), Flow resistance in gravel-bed rivers, *J. Hydraul. Div. Am. Soc. Civ. Eng.*, *105*, 365–379.

Hygelund, B., and M. Manga (2003), Field measurements of drag coefficients for model large woody debris, *Geomorphology*, *51*, 175–185.

Jarrett, R. D. (1984), Hydraulics of high-gradient streams, *J. Hydraul. Eng.*, *110*(11), 1519–1539.

Katul, G., P. Wiberg, J. Albertson, and G. Hornberger (2002), A mixing layer theory for flow resistance in shallow streams, *Water Resour. Res.*, *38*(11), 1250, doi:10.1029/2001WR000817.

Keulegan, G. H. (1938), Laws of turbulent flow in open channels, *J. Res. Natl. Bur. Stand.*, *21*, 707–741.

Kutner, M. H., C. J. Nachtsheim, J. Neter, and W. Li (2005), *Applied Linear Statistical Models*, 1396 pp., McGraw-Hill, Irwin, N. Y.

Lawrence, D. S. L. (1997), Macroscale surface roughness and frictional resistance in overland flow, *Earth Surf. Processes Landforms*, *22*, 365–382.

Lawrence, D. S. L. (2000), Hydraulic resistance in overland flow during partial and marginal surface inundation: Experimental observations and modeling, *Water Resour. Res.*, *36*, 2381–2393, doi:10.1029/2000WR900095.

Lee, A. J., and R. I. Ferguson (2002), Velocity and flow resistance in step-pool streams, *Geomorphology*, *46*, 59–71.

Legleiter, C. J., T. L. Phelps, and E. E. Wohl (2007), Geostatistical analysis of the effects of stage and roughness on reach-scale spatial patterns of velocity and turbulence intensity, *Geomorphology*, *83*, 322–345.

Leica Geosystems (2008), *Cyclone 5.8.1.: Comprehensive software for working with laser scan data*, Leica Geosystems HDS LLC, San Ramon, CA.

Limerinos, J. T. (1970), Determination of the Manning coefficient for measured bed roughness in natural channels, *U.S. Geol. Surv. Water Supply Pap. 1898-B*, U.S. Geol. Surv., Washington, D. C.

Magirl, C. S., J. W. Gartner, G. M. Smart, and R. H. Webb (2009), Water velocity and the nature of critical flow in large rapids on the Colorado River, Utah, *Water Resour. Res.*, *45*, W05427, doi:10.1029/2009WR007731.

Manga, M., and J. W. Kirchner (2000), Stress partitioning in streams by large woody debris, *Water Resour. Res.*, *36*, 2373–2379, doi:10.1029/2000WR900153.

Manners, R. B., M. W. Doyle, and M. J. Small (2007), Structure and hydraulics of natural woody debris jams, *Water Resour. Res.*, *43*, W06432, doi:10.1029/2006WR004910.

Maxwell, A. R., and A. N. Papanicolaou (2001), Step-pool morphology in high-gradient streams, *Int. J. Sediment Res.*, *72*, 99–108.

Millar, R. G. (1999), Grain and form resistance in gravel-bed rivers, *J. Hydraul. Res.*, *37*, 303–312.

Millar, R. G., and M. C. Quick (1994), Flow resistance of high-gradient gravel channels, in *Hydraulic Engineering '94 ASCE*, edited by G. V. Cotroneo and R. R. Rumer, pp. 717–721, Buffalo, N. Y.

Montgomery, D. R., and J. M. Buffington (1997), Channel-reach morphology in mountain drainage basins, *Geol. Soc. Am. Bull.*, *109*, 596–611.

Nelson, J. M., S. R. McLean, and S. R. Wolfe (1993), Mean flow and turbulence fields over two-dimensional bed forms, *Water Resour. Res.*, *29*, 3935–3953, doi:10.1029/93WR01932.

Pagliara, S., and P. Chiavaccini (2006), Flow resistance of rock chutes with protruding boulders, *J. Hydraul. Eng.*, *132*, 545–552.

Parker, G., and A. W. Peterson (1980), Bar resistance of gravel-bed streams, *J. Hydraul. Div. Am. Soc. Civ. Eng.*, *106*, 1559–1573.

Prestegaard, K. L. (1983), Bar resistance in gravel bed streams at bankfull stage, *Water Resour. Res.*, *19*(2), 472–476, doi:10.1029/WR019i002p00472.

Reid, D. E., and E. J. Hickin (2008), Flow resistance in steep mountain streams, *Earth Surf. Processes Landforms*, *33*, 2211–2240, doi:10.1002/esp.1682.

Rickenmann, D. (1991), Hyperconcentrated flow and sediment transport at steep slopes, *J. Hydraul. Eng.*, *117*, 1419–1439.

Rouse, H. (1965), Critical analysis of open-channel resistance, *J. Hydraul. Div. Am. Soc. Civ. Eng.*, *91*, 1–25.

Shields, A. (1936), Application of similarity principles and turbulence research to bed-load movement. *Mitteilunger der Preussischen Versuchsanstalt für Wasserbau und Schiffbau*, *26*, 5–24.

Shields, F. D., Jr., and C. J. Gippel (1995), Prediction of effects of woody debris removal on flow resistance, *J. Hydraul. Eng.*, *121*, 341–354.

Smart, G. M., M. J. Duncan, J. M. Walsh (2002), Relatively rough flow resistance equations, *J. Hydraul. Eng.*, *128*, 568–578.

Thorne, C. R., and L. W. Zevenbergen (1985), Estimating mean velocity in mountain rivers, *J. Hydraul. Eng.*, *111*, 612–624.

Wallerstein, N. P., C. V. Alonso, S. J. Bennett, and C. R. Thorne (2002), Surface wave forces acting on submerged logs, *J. Hydraul. Eng.*, *128*, 349–353.

Wiberg, P. L., and J. D. Smith (1991), Velocity distribution and bed roughness in high-gradient streams, *Water Resour. Res.*, *23*, 1471–1480, doi:10.1029/90WR02770.

Wilcox, A. C., and E. E. Wohl (2006), Flow resistance dynamics in step-pool stream channels: 1. Large woody debris and controls on total resistance, *Water Resour. Res.*, *42*, W05418, doi:10.1029/2005WR004277.

Wilcox, A. C., and E. E. Wohl (2007), Field measurements of three-dimensional hydraulics in a step-pool channel, *Geomorphology*, *83*, 215–231, doi:10.1016/j.geomorph.2006.02.017.

Wilcox, A. C., J. M. Nelson, and E. E. Wohl (2006), Flow resistance dynamics in step-pool channels: 2. Partitioning between grain, spill, and woody debris resistance, *Water Resour. Res.*, *42*, W05419, doi:10.1029/2005WR004278.

Wohl, E. E., and H. Ikeda (1998), The effect of roughness configuration on velocity profiles in an artificial channel, *Earth Surf. Processes Landforms*, *23*, 159–169.

Wohl, E. E., and D. M. Thompson (2000), Velocity characteristics along a small step-pool channel, *Earth Surf. Processes Landforms*, *25*, 353–367.

Young, W. J. (1991), Flume study of the hydraulic effects of large woody debris in lowland rivers, *Reg. Rivers Res. Manage.*, *6*, 203–211.

Zimmerman, A. (2010), Flow resistance in steep streams: An experimental study, *Water Resour. Res.*, *46*, W09536, doi:10.1029/2009WR007913.

Zimmerman, A., and M. Church (2001), Channel morphology, gradient profiles and bed stresses during flood in a step-pool channel, *Geomorphology*, *40*, 311–327.

B. P. Bledsoe and S. E. Yochum, Department of Civil and Environmental Engineering, Colorado State University, Fort Collins, CO 80523, USA. (brian.bledsoe@engr.colostate.edu; yochum@rams.colostate.edu)

G. C. L. David and E. Wohl, Department of Geosciences, Colorado State University, Fort Collins, CO 80523, USA. (gcldavid@lamar.colostate.edu; ellenw@warnercnr.colostate.edu)